

Leading order infrared quantum chromodynamics in Coulomb gauge

P. Watson and H. Reinhardt
*Institut für Theoretische Physik, Universität Tübingen,
 Auf der Morgenstelle 14, D-72076 Tübingen, Deutschland*

A truncation scheme for the Dyson-Schwinger equations of quantum chromodynamics in Coulomb gauge within the first order formalism is presented. The truncation is based on an Ansatz for the Coulomb kernel occurring in the action. Results at leading loop order and in the infrared are discussed for both the Yang-Mills and quark sectors. It is found that the resulting equations for the static gluon and quark propagators agree with those derived in a quasi-particle approximation to the canonical Hamiltonian approach. Moreover, a connection to the heavy quark limit is established. The equations are analyzed numerically and it is seen that in both the gluonic and quark sectors, a nontrivial dynamical infrared mass scale emerges.

PACS numbers: 11.15.-q, 12.38.Aw

I. INTRODUCTION

Confinement and the dynamical breaking of chiral symmetry are two highly nontrivial, nonperturbative aspects of the hadron spectrum. Ideally, we would like to understand both from first principles calculations of the underlying gauge theory which is quantum chromodynamics (QCD). Because both effects are manifested in the infrared regime (and where singularities may occur), nonperturbative continuum functional methods are one framework within which to study the problem. In such studies, one is invariably forced to choose a gauge and our choice is Coulomb gauge. One initial reason for this choice is that there exists an appealing picture for confinement: the Gribov-Zwanziger scenario [1–3].

Coulomb gauge studies of QCD have become an area of increasing importance in recent years, mainly due to progress within the canonical Hamiltonian approach (see, for example, Refs. [4–11] and references therein), although such studies have been around for quite some time (e.g., Refs. [12, 13]). The essential idea is that given the Hamilton operator [14] and an Ansatz for the ground state vacuum wavefunctional (supplemented with Gauss' law), the variational principle can then be used to generate equations for the various Green's functions of the theory. For a given Ansatz, the resulting equations are exact.

A second approach to nonperturbative QCD in Coulomb gauge (and that considered here) is to study the Dyson-Schwinger equations [15]. In contrast to the canonical approach, Dyson-Schwinger studies in Coulomb gauge are far less developed mainly due to their inherent technical challenges (although attempts have been made [16, 17]). This being said, various facets of the formalism have been understood: their one-loop perturbative behavior [18–20], the Slavnov-Taylor identities [21], the emergence of a nonperturbative constraint on the total charge [22] and the case of heavy quarks [23–25]. The standard Dyson-Schwinger approach is distinct from the canonical approach in two primary respects: it includes the energy dependence of the Green's functions from the outset and must therefore deal directly with the noncovariance of Coulomb gauge; also, truncations are typically made to the individual terms in the (full) equations.

Clearly, it is desirable to be able to connect the canonical Hamiltonian and Dyson-Schwinger formalisms. Working in concert, the two different formulations can mutually reinforce each other – what is difficult in one may be intuitive in the other and vice versa. An initial aim of this paper is thus to show how the gap equations for the static gluon and quark propagators, obtained originally within the canonical formalism [6, 12], can be derived from a leading order truncation of the Dyson-Schwinger equations. This truncation treats quarks and gluons on an equal footing. It also takes into account the nonperturbative constraint that the total color charge be conserved and vanishing [22]. Moreover, the connection to the known Coulomb gauge heavy quark limit [23–25] can be established. The gap equations will be analyzed numerically for a particular nonperturbative input and various aspects will be explored. In the case of the gluon sector, it will be seen that a nontrivial dynamical mass scale emerges and which is connected to the nonperturbative renormalization of the theory. For the quark sector, both the dynamical chiral symmetry breaking and the heavy quark limit will be discussed.

The paper is organized as follows. We begin in Sec. II by introducing the first order formalism, including the total color charge constraint that arises from the resolution of the temporal zero modes inherent to Coulomb gauge. The Dyson-Schwinger equations and the leading order truncation scheme will be presented in Sec. III. The analytic development of the Dyson-Schwinger equations, in particular the reduction to the static equations and the heavy quark limit, is given in Sec. IV. Numerical results for both the gluonic and quark sectors appear in Sec. V. We close the paper with a summary and discussion.

II. FIRST ORDER FORMALISM

To begin, let us consider the generating functional integral and action for QCD and review various aspects of the first order formalism in Coulomb gauge. The description initially follows closely in the spirit of Refs. [3, 15, 22, 26]. The generating functional is written as

$$Z[\rho, \vec{J}, \vec{\chi}, \chi] = \int \mathcal{D}\Phi \exp \left\{ \imath \mathcal{S}_{QCD} + \imath \int dx \left[\rho_x^a \sigma_x^a + \vec{J}_x^a \cdot \vec{A}_x^a + \vec{\chi}_{\alpha x} q_{\alpha x} + \bar{q}_{\alpha x} \chi_{\alpha x} \right] \right\} \quad (2.1)$$

where $\mathcal{D}\Phi$ generically represents the functional integral measure over all fields present, with sources $\rho, \vec{J}, \vec{\chi}, \chi$ for the various gluon and quark fields (see below). In this section, only the source ρ will be relevant to the discussion and so we set $\vec{J} = \vec{\chi} = \chi = 0$. The (Minkowski space) QCD action reads

$$\mathcal{S}_{QCD} = \int dx \left\{ \bar{q}_{\alpha x} \left[\imath \gamma^0 D_{0x} + \imath \vec{\gamma} \cdot \vec{D}_x - m \right]_{\alpha\beta} q_{\beta x} + \frac{1}{2} \vec{E}_x^a \cdot \vec{E}_x^a - \frac{1}{2} \vec{B}_x^a \cdot \vec{B}_x^a \right\}. \quad (2.2)$$

In the above, $(\bar{q}) q_{\beta x}$ represents the (conjugate) quark field with fundamental color, spin and flavor indices collectively denoted with the index β and position argument denoted with subscript x . The Dirac γ -matrices obey the Clifford algebra $\{\gamma^\mu, \gamma^\nu\} = 2g^{\mu\nu}$ with metric $g^{\mu\nu} = \text{diag}(1, -\vec{1})$ (we explicitly extract all minus signs associated with the metric such that the components of spatial vectors such as \vec{x} are written with subscripts, i.e., x_i). The temporal and spatial components of the covariant derivative in the fundamental color representation are

$$\begin{aligned} D_{0x} &= \partial_{0x} - \imath g \sigma_x^a = \partial_{0x} - \imath g \sigma_x^a T^a, \\ \vec{D}_x &= \vec{\nabla}_x + \imath g \vec{A}_x = \vec{\nabla}_x + \imath g \vec{A}_x^a T^a \end{aligned} \quad (2.3)$$

where σ_x^a and \vec{A}_x^a are the temporal and spatial components of the gluon field, respectively, and where the superscript a denotes the color index in the adjoint representation. The generators T^a obey $[T^a, T^b] = \imath f^{abc} T^c$, where the f^{abc} are the structure constants and we use the normalization $\text{Tr}[T^a T^b] = \delta^{ab}/2$. The chromoelectric and chromomagnetic fields are written in terms of the gluon field as

$$\begin{aligned} \vec{E}_x^a &= -\partial_{0x} \vec{A}_x^a - \vec{D}_x^{ab} \sigma_x^b, \\ \vec{B}_x^a &= \vec{\nabla}_x \times \vec{A}_x^a - \frac{1}{2} g f^{abc} \vec{A}_x^b \times \vec{A}_x^c \end{aligned} \quad (2.4)$$

with the spatial component of the covariant derivative in the adjoint color representation given by

$$\vec{D}_x^{ab} = \delta^{ab} \vec{\nabla}_x - g f^{acb} \vec{A}_x^c. \quad (2.5)$$

The QCD action is invariant under gauge transforms of the type

$$\begin{aligned} \sigma &\rightarrow \sigma^\theta = U \sigma U^\dagger - \frac{\imath}{g} (\partial_0 U) U^\dagger, \\ \vec{A} &\rightarrow \vec{A}^\theta = U \vec{A} U^\dagger + \frac{\imath}{g} (\vec{\nabla} U) U^\dagger, \\ q &\rightarrow q^\theta = U q \end{aligned} \quad (2.6)$$

where $U_x = \exp \{-\imath \theta_x^a T^a\}$ is a spacetime dependent element of the $SU(N_c)$ group. Because of this invariance, the functional integral (in the absence of sources) contains a divergence by virtue of the integration over the gauge group. Whilst this is in principle a global factor which can be absorbed into the normalization, when calculating Green's functions it leads to the necessity for fixing the gauge. This is typically achieved in the continuum formalism via the Faddeev-Popov technique which involves inserting the following identity into the functional integral:

$$1 = \int \mathcal{D}\theta \delta \left(F \left[\sigma^\theta, \vec{A}^\theta \right] \right) \text{Det} \left[M^{ab}(x, y) \right], \quad M^{ab}(x, y) = \left. \frac{\delta F^a \left[\sigma_x^\theta, \vec{A}_x^\theta \right]}{\delta \theta_y^b} \right|_{F=0}. \quad (2.7)$$

The expression $F[\sigma, \vec{A}]$ determines the gauge condition ($F = 0$) and we choose Coulomb gauge:

$$F[\sigma, \vec{A}] := \vec{\nabla} \cdot \vec{A}, \quad (2.8)$$

for which the Faddeev-Popov kernel reads

$$M^{ab}(x, y) \sim -\vec{\nabla} \cdot \vec{D}_x^{ab} \delta(x - y). \quad (2.9)$$

There are caveats to the identity Eq. (2.7), namely that when the gauge fixing is incomplete, zero modes of the Faddeev-Popov operator will arise and one encounters the Gribov problem [1]. In Coulomb gauge there is a special case: temporal zero modes corresponding to time dependent but spatially independent gauge transforms [22], arising because the Faddeev-Popov operator involves only spatial differential operators, and for which

$$-\vec{\nabla} \cdot \vec{D}_x^{ab} \theta^b(x_0) = 0. \quad (2.10)$$

Clearly, such zero eigenvalues (there are $N_c^2 - 1$ of them at each time x_0) for the Faddeev-Popov operator automatically result in a vanishing functional determinant and hence invalidate the identity Eq. (2.7). In this work, we shall not consider the more general case of spatially dependent zero modes (which lead to the existence of Gribov copies in the usual sense). Following [22], we modify the original identity to

$$\mathbb{1} = \int \mathcal{D}\bar{\theta} \delta \left(F \left[\sigma^\theta, \bar{A}^\theta \right] \right) \overline{\text{Det}} \left[M^{ab}(x, y) \right] \quad (2.11)$$

where $\mathcal{D}\bar{\theta}$ explicitly excludes the temporal zero modes $\theta(x_0)$ and

$$\overline{\text{Det}} \left[M^{ab}(x, y) \right] = \text{Det} \left[M^{ab}(x, y) \right]_{-\vec{\nabla} \cdot \vec{D} \theta \neq 0} \quad (2.12)$$

is the determinant with such zero modes removed. Replacing the source term (ρ) for the temporal gluon field in the functional integral (as mentioned, the other sources play no role in this section and are set to zero), the generating functional for Coulomb gauge QCD is thus written

$$Z[\rho] = \int \mathcal{D}\Phi \delta \left(\vec{\nabla} \cdot \vec{A} \right) \overline{\text{Det}} \left[-\vec{\nabla} \cdot \vec{D} \right] \exp \left\{ \imath \mathcal{S}_{QCD} + \imath \int dx \rho_x^a \sigma_x^a \right\}. \quad (2.13)$$

To proceed, it is useful to convert to the first order formalism [3, 15, 22]. This is achieved by introducing an auxiliary vector field ($\vec{\pi}$), noting the following functional integral identity for the chromoelectric part of the action:

$$\exp \left\{ \imath \int dx \frac{1}{2} \vec{E}_x^a \cdot \vec{E}_x^a \right\} = \int \mathcal{D}\vec{\pi} \exp \left\{ \imath \int dx \left[-\frac{1}{2} \vec{\pi}_x^a \cdot \vec{\pi}_x^a - \vec{\pi}_x^a \cdot \vec{E}_x^a \right] \right\}. \quad (2.14)$$

The new field is then split into components using

$$\text{const} = \int \mathcal{D}\phi \mathcal{D}\tau \exp \left\{ -\imath \int dx \tau_x^a \left(\vec{\nabla}_x \cdot \vec{\pi}_x^a + \vec{\nabla}_x^2 \phi_x^a \right) \right\}, \quad (2.15)$$

changing variables $\vec{\pi} \rightarrow \vec{\pi} - \vec{\nabla} \phi$ and integrating out the Lagrange multiplier. The generating functional now reads

$$Z[\rho] = \int \mathcal{D}\Phi \delta \left(\vec{\nabla} \cdot \vec{A} \right) \delta \left(\vec{\nabla} \cdot \vec{\pi} \right) \overline{\text{Det}} \left[-\vec{\nabla} \cdot \vec{D} \right] e^{\imath \mathcal{S}} \quad (2.16)$$

with the action

$$\begin{aligned} \mathcal{S} &= \mathcal{S}_q + \mathcal{S}' + \mathcal{S}_\sigma, \\ \mathcal{S}_q &= \int dx \bar{q}_{\alpha x} \left[\imath \gamma^0 \partial_{0x} + \imath \vec{\gamma} \cdot \vec{D} - m \right]_{\alpha\beta} q_{\beta x}, \\ \mathcal{S}' &= \int dx \left[-\frac{1}{2} \vec{B}_x^a \cdot \vec{B}_x^a - \frac{1}{2} \vec{\pi}_x^a \cdot \vec{\pi}_x^a + \vec{\pi}_x^a \cdot \partial_{0x} \vec{A}_x^a + \frac{1}{2} \phi_x^a \vec{\nabla}_x^2 \phi_x^a \right], \\ \mathcal{S}_\sigma &= \int dx \sigma_x^a \left(\vec{\nabla}_x \cdot \vec{D}_x^{ab} \phi_x^b + \rho_x^a + g f^{abc} \vec{A}_x^b \cdot \vec{\pi}_x^c + g \bar{q}_{\alpha x} [\gamma^0 T^a]_{\alpha\beta} q_{\beta x} \right). \end{aligned} \quad (2.17)$$

Were the δ -functional constraints written in terms of Lagrange multiplier fields, the determinant written in terms of ghosts and sources for all fields present, the theory would be in a local form suitable for discussing perturbation

theory as in Refs. [15, 18, 20]. The important feature about the decomposition to the first order formalism is that the action is now linear in σ , which can be integrated out to give

$$Z[\rho] = \int \mathcal{D}\Phi \delta(\vec{\nabla} \cdot \vec{A}) \delta(\vec{\nabla} \cdot \vec{\pi}) \overline{\text{Det}}[-\vec{\nabla} \cdot \vec{D}] \delta(\vec{\nabla} \cdot \vec{D}\phi + \vec{\rho}) e^{(\imath \mathcal{S}_q + \imath \mathcal{S}')} \quad (2.18)$$

where

$$\vec{\rho}_x^a = \rho_x^a + g f^{abc} \vec{A}_x^b \cdot \vec{\pi}_x^c + g \vec{q}_{\alpha x} [\gamma^0 T^a]_{\alpha\beta} q_{\beta x}. \quad (2.19)$$

The ϕ field can be integrated out by using the eigenfunctions of the Faddeev-Popov operator as a complete orthonormal basis for an expansion, the crucial point being that one must take into account the existence of the temporal zero modes. Following Ref. [22], the result is

$$\int \mathcal{D}\phi \delta(\vec{\nabla} \cdot \vec{D}\phi + \vec{\rho}) \exp \left\{ \imath \int dx \frac{1}{2} \phi_x^a \vec{\nabla}_x^2 \phi_x^a \right\} = \delta \left(\int d\vec{x} \vec{\rho} \right) \overline{\text{Det}}[-\vec{\nabla} \cdot \vec{D}]^{-1} \exp \left\{ -\imath \int dx \frac{1}{2} \vec{\rho}_x^a \hat{F}_x^{ab} \vec{\rho}_x^b \right\} \quad (2.20)$$

where

$$\hat{F}_x^{ab} = \left[-\vec{\nabla}_x \cdot \vec{D}_x^{ac} \right]^{-1} \left(-\vec{\nabla}_x^2 \right) \left[-\vec{\nabla}_x \cdot \vec{D}_x^{cb} \right]^{-1}. \quad (2.21)$$

The δ -functional constraint that emerges constrains the total color charge, the spatial integral arising from the projection onto the temporal zero mode. The generating functional is now,

$$Z[\rho] = \int \mathcal{D}\Phi \delta(\vec{\nabla} \cdot \vec{A}) \delta(\vec{\nabla} \cdot \vec{\pi}) \delta \left(\int d\vec{x} \vec{\rho} \right) e^{(\imath \mathcal{S}_q + \imath \mathcal{S})}, \quad (2.22)$$

with the action term

$$\mathcal{S} = \int dx \left[-\frac{1}{2} \vec{B}_x^a \cdot \vec{B}_x^a - \frac{1}{2} \vec{\pi}_x^a \cdot \vec{\pi}_x^a + \vec{\pi}_x^a \cdot \partial_{0x} \vec{A}_x^a - \frac{1}{2} \vec{\rho}_x^a \hat{F}_x^{ab} \vec{\rho}_x^b \right]. \quad (2.23)$$

Some comments are in order. The (modified) Faddeev-Popov determinant in the generating functional cancels exactly, which is equivalent to saying that Coulomb gauge is ghost-free and this arises from the elimination of the temporal gluon field. Notice though that the inverse Faddeev-Popov operator still plays a role. What is left of the gluon sector concerns the two spatially transverse vector fields \vec{A} and $\vec{\pi}$ ($\vec{\pi}$ would classically correspond to the momentum conjugate of \vec{A}) which in quantum electrodynamics would give rise to the two physical transverse polarization states of the photon. The remnant δ -functional constraint is the statement that the total color charge of the system must be conserved and vanishing and this explicitly includes a contribution from the external source ρ , the gluon field and the quark term. This is nothing other than the application of Gauss' law.

In order to make sense of the generating functional, Eq. (2.22), the δ -functional constraint on the total charge must be rewritten in a useful form. This is most conveniently done with a Gaussian form:

$$\delta \left(\int d\vec{x} \vec{\rho} \right) \sim \lim_{\mathcal{C} \rightarrow \infty} \mathcal{N}(\mathcal{C}) \exp \left\{ -\frac{\imath}{2} \int dy dz \vec{\rho}^a(y) \mathcal{C} \delta^{ab} \delta(y_0 - z_0) \vec{\rho}^b(z) \right\} \quad (2.24)$$

where \mathcal{C} is a constant, $\mathcal{N}(\mathcal{C})$ is a normalization factor (that will be henceforth included implicitly in the functional integral measure) and the limit $\mathcal{C} \rightarrow \infty$ will be taken only at the end of any calculation. The generating functional can thus be written in the form

$$Z[\rho] \sim \lim_{\mathcal{C} \rightarrow \infty} \int \mathcal{D}\Phi \delta(\vec{\nabla} \cdot \vec{A}) \delta(\vec{\nabla} \cdot \vec{\pi}) \exp \{ \imath \mathcal{S}'' \} \exp \left\{ -\frac{\imath}{2} \int dy dz \vec{\rho}^a(y) [F^{ab}(y_0; \vec{y}, \vec{z}) + \mathcal{C} \delta^{ab}] \delta(y_0 - z_0) \vec{\rho}^b(z) \right\} \quad (2.25)$$

where

$$\mathcal{S}'' = \mathcal{S}_q + \int dx \left[-\frac{1}{2} \vec{B}_x^a \cdot \vec{B}_x^a - \frac{1}{2} \vec{\pi}_x^a \cdot \vec{\pi}_x^a + \vec{\pi}_x^a \cdot \partial_{0x} \vec{A}_x^a \right] \quad (2.26)$$

and

$$F^{ab}(y_0; \vec{y}, \vec{z}) = \hat{F}_y^{ab} \delta(\vec{y} - \vec{z}). \quad (2.27)$$

We shall refer to F as the Coulomb kernel. F is defined at each time, y_0 , since it involves no temporal operators. We see that the effect of the total charge conservation constraint is the presence of a potentially ill-defined and divergent constant additive term to the Coulomb kernel. It will be seen later that the constant, \mathcal{C} , cancels out when considering physical quantities.

As noted in Ref. [26], the Coulomb kernel is intimately related to the temporal gluon propagator. Although the temporal gluon field has been integrated out, the propagator still exists as a functional second derivative of $Z[\rho]$ (this is why we have so far retained the source) and is defined in configuration space as

$$W_{\sigma\sigma}^{cd}(v, w) = \frac{1}{Z[\rho]} \frac{\delta^2 Z[\rho]}{\delta \iota \rho_v^c \delta \iota \rho_w^d} \Big|_{\rho=0}. \quad (2.28)$$

The temporal gluon propagator is known perturbatively in both the first and second order Coulomb gauge formalisms [18, 19]. Indeed, since the manipulations involved in going from the second to first order formalisms are integral identities performed on the generating functional, the spatial and temporal gluon propagators are identical in both formalisms. Taking two functional derivatives of Z given by Eq. (2.25) with respect to the source ρ and subsequently setting $\rho = 0$, one obtains:

$$\begin{aligned} W_{\sigma\sigma}^{cd}(v, w) &= \frac{1}{Z[0]} \int \mathcal{D}\Phi \delta(\vec{\nabla} \cdot \vec{A}) \delta(\vec{\nabla} \cdot \vec{\pi}) \exp\{\iota \mathcal{S}''\} \\ &\times \lim_{\mathcal{C} \rightarrow \infty} \exp\left\{-\frac{\iota}{2} \int dy dz \hat{\rho}^a(y) [F^{ab}(y_0; \vec{y}, \vec{z}) + \mathcal{C} \delta^{ab}] \delta(y_0 - z_0) \hat{\rho}^b(z)\right\} \\ &\times \left\{\iota [F^{cd}(v_0; \vec{v}, \vec{w}) + \mathcal{C} \delta^{cd}] \delta(v_0 - w_0) + \int d\vec{y} [F^{ce}(v_0; \vec{v}, \vec{y}) + \mathcal{C} \delta^{ce}] \hat{\rho}^e(v_0, \vec{y}) \int d\vec{z} [F^{df}(w_0; \vec{w}, \vec{z}) + \mathcal{C} \delta^{df}] \hat{\rho}^f(w_0, \vec{z})\right\} \end{aligned} \quad (2.29)$$

where

$$\hat{\rho}_x^a = g f^{abc} \vec{A}_x^b \cdot \vec{\pi}_x^c + g \vec{q}_{\alpha x} [\gamma^0 T^a]_{\alpha\beta} q_{\beta x}. \quad (2.30)$$

Were it not for the δ -functional constraint on the total charge, this expression would be the same as in Ref. [26] and the conclusion would be that the temporal gluon propagator splits into two parts, instantaneous and non-instantaneous:

$$W_{\sigma\sigma}^{cd}(v, w) \sim \langle \iota F^{cd}(v_0; \vec{v}, \vec{w}) \rangle \delta(v_0 - w_0) + \langle [F_v^{ce} \hat{\rho}^e(v_0, \vec{v})] [F_w^{df} \hat{\rho}^f(w_0, \vec{w})] \rangle, \quad (2.31)$$

the instantaneous part being the expectation value of the Coulomb kernel and arising because the original Faddeev-Popov operator involves only spatial operators. However, the presence of the total charge constraint alters this: in particular, noting that the additional term is independent of the fields, we see that the instantaneous part of the temporal gluon propagator has the form

$$W_{\sigma\sigma}^{cd}(v, w)^{\text{inst}} \sim \langle \iota F^{cd}(v_0; \vec{v}, \vec{w}) \rangle \delta(v_0 - w_0) + \lim_{\mathcal{C} \rightarrow \infty} \iota \mathcal{C} \delta^{cd} \delta(v_0 - w_0) \quad (2.32)$$

(in the original term involving the expectation value of F , the $\mathcal{C} \rightarrow \infty$ limit merely serves to reinstate the δ -functional charge constraint in the definition of the functional integral). The interpretation of the new term is simple: it is simply a (divergent) spatial constant and is completely nonperturbative in origin. As mentioned before, to make sense of the divergence, we shall consider \mathcal{C} as being finite until the last step of any calculation.

III. DYSON-SCHWINGER EQUATIONS AND TRUNCATION

Let us discuss the Dyson-Schwinger equations and their truncation. The techniques involved in the derivation of the Dyson-Schwinger equations are standard, such that we shall present here only the most salient points in the interests of readability. The reader is referred to Refs. [15, 19, 20] for an explicit account of the derivation of such Dyson-Schwinger equations in Coulomb gauge. Noticing that the Coulomb kernel occurring in the action cannot be written as a finite order polynomial in the fields (due to the presence of the *inverse* Faddeev-Popov operator, this term is nonlocal), we must make some form of approximation in order to apply the standard Dyson-Schwinger formalism. To this end, we will introduce and justify a leading order truncation, whereby the Coulomb kernel occurring in the action is replaced by its expectation value and which will serve as an input into the resulting equations.

To start, let us consider the generating functional, Eq. (2.25), in the absence of sources. By implementing the transversality constraints on \vec{A} , $\vec{\pi}$ via Lagrange multiplier fields (λ, τ , respectively), the functional integral and corresponding action can be written

$$Z = \int \mathcal{D}\Phi e^{\mathcal{S}}, \quad \mathcal{S} = \mathcal{S}^2 + \mathcal{S}^3 + \mathcal{S}^4 \quad (3.1)$$

where

$$\begin{aligned} \mathcal{S}^2 &= \int dx \left\{ \bar{q}_{\alpha x} \left[\imath \gamma^0 \partial_{0x} + \imath \vec{\gamma} \cdot \vec{\nabla}_x - m \right]_{\alpha\beta} q_{\beta x} + \frac{1}{2} A_{ix}^a \left[\vec{\nabla}_x^2 \delta_{ij} - \nabla_{ix} \nabla_{jx} \right] A_{jx}^a \right. \\ &\quad \left. - \frac{1}{2} \pi_{ix}^a \pi_{ix}^a + \pi_{ix}^a \partial_{0x} A_{ix}^a - \lambda_x^a \nabla_{jx} A_{jx}^a - \tau_x^a \nabla_{jx} \pi_{jx}^a \right\}, \\ \mathcal{S}^3 &= \int dx dy dz \left\{ -g [T^a \gamma_i]_{\alpha\beta} \delta(x-y) \delta(x-z) \bar{q}_{\alpha x} A_{iy}^a q_{\beta z} + g f^{abc} [\nabla_{jx} \delta(x-z)] \delta(x-y) A_{kz}^a A_{jx}^b A_{ky}^c \right\}, \\ \mathcal{S}^4 &= -\frac{1}{2} g^2 \int dx dy \left[f^{ade} A_{ix}^d \pi_{ix}^e + [\gamma^0 T^a]_{\alpha\beta} \bar{q}_{\alpha x} q_{\beta y} \right] \tilde{F}^{ab}(x, y; \vec{A}) \left[f^{bfg} A_{jy}^f \pi_{jy}^g + [\gamma^0 T^b]_{\gamma\delta} \bar{q}_{\gamma y} q_{\delta y} \right] \\ &\quad - \frac{1}{4} g^2 f^{abc} f^{ade} \int dx A_{ix}^b A_{jx}^c A_{ix}^d A_{jx}^e, \end{aligned} \quad (3.2)$$

and where (recognizing the \vec{A} -dependence of the covariant derivative, \vec{D} , given by Eq. (2.5))

$$\begin{aligned} \tilde{F}^{ab}(x, y; \vec{A}) &= [F^{ab}(x_0; \vec{x}, \vec{y}) + \mathcal{C} \delta^{ab}] \delta(x_0 - y_0) \\ &= \left[-\vec{\nabla}_x \cdot \vec{D}_x^{ac} \right]^{-1} \left(-\vec{\nabla}_x^2 \right) \left[-\vec{\nabla}_x \cdot \vec{D}_x^{cb} \right]^{-1} \delta(x - y) + \mathcal{C} \delta^{ab} \delta(x_0 - y_0). \end{aligned} \quad (3.3)$$

Knowing that the Dyson-Schwinger equations are formed via functional derivatives of the generating functional, we observe that the \vec{A} -dependence occurring within \tilde{F} always comes with an associated factor of the coupling, such that explicit functional derivatives of \tilde{F} will always result in additional loop structure. As a leading (loop) order Ansatz, we therefore make the following truncation for the Coulomb kernel:

$$\tilde{F}^{ab}(x, y; \vec{A}) \rightarrow \tilde{F}^{ab}(x, y) = [F(\vec{x} - \vec{y}) + \mathcal{C}] \delta^{ab} \delta(x_0 - y_0) \quad (3.4)$$

where F is some scalar function which will serve as a nonperturbative input to the system of Dyson-Schwinger equations (the explicit expression will be discussed later). The Coulomb kernel is instantaneous (as is its expectation value) so that in momentum space, the function F will be independent of energy:

$$\tilde{F}^{ab}(x, y) = \int \bar{d}k e^{-\imath k \cdot (x-y)} \tilde{F}^{ab}(k) \sim \int \bar{d}k e^{-\imath k \cdot (x-y)} \delta^{ab} \left[F(\vec{k}^2) + \mathcal{C} (2\pi)^3 \delta(\vec{k}) \right] \quad (3.5)$$

where $\bar{d}k = d^4k / (2\pi)^4$. It is clear from the discussion of the last section that \tilde{F} is intimately related to the instantaneous part of the dressed temporal gluon propagator. The tree-level contribution to \tilde{F} is $\sim (-\vec{\nabla}^2)^{-1}$ (or $1/\vec{k}^2$ in momentum space), i.e., independent of \vec{A} and so the one-loop perturbative results are in principle preserved within this Ansatz.

Before continuing, it is worth briefly contrasting the formalism above with those of previous studies, namely Refs. [15, 20]. These studies focused on a local form of the Coulomb gauge first order formalism, whereby the σ and ϕ fields were not integrated out and the Faddeev-Popov determinant was written in terms of ghost fields. This form is ideal for studying perturbation theory. Here, after integrating out the σ and ϕ fields, the Faddeev-Popov determinant cancels, leaving a form for the action involving the nonlocal Coulomb interaction term $\rho \tilde{F} \rho$. The purely spatial gluonic and quark components of the action (i.e., those that exclusively involve only the \vec{A} , $\vec{\pi}$, \bar{q} and q fields) are unaltered, meaning that many of the previous results from Refs. [15, 20] pertaining to these components are retained. After replacing \tilde{F} with its expectation value (which serves as an external input into the system), the Coulomb interaction term involves three new momentum dependent tree-level interactions between the \vec{A} , $\vec{\pi}$ and quark fields (their explicit forms will be presented shortly). These new interaction terms replace the dynamical interaction content of the σ , ϕ and ghost degrees of freedom with a simple set of effective vertices. In effect, the full nonperturbative towers of Dyson-Schwinger equations involving the σ , ϕ and ghost fields have been ‘solved’ by the Ansatz for \tilde{F} . Obviously, this ‘solution’ is only a leading order Ansatz; we shall however see that important nonperturbative physics is nonetheless

contained. As has been seen, the removal of the σ , ϕ and ghost fields in the nonlocal formalism is intimately related to the imposal of Gauss' law and (total) charge conservation; in the local formulation, the Slavnov-Taylor identities perform this role [21].

The Dyson-Schwinger equations are integral equations relating the various proper (one-particle irreducible, [1PI]) Green's functions of the theory. The most basic of the 1PI functions are the two-point proper functions and in the current formalism, with only \vec{A} , $\vec{\pi}$ and quark fields (aside from the trivial Lagrange multiplier fields), the most general momentum space decomposition of these is given by (see Refs. [15, 20] for details of the derivation and notation)

$$\begin{aligned}\Gamma_{\pi\pi ij}^{ab}(k) &= i\delta^{ab} \left[\delta_{ij} \Gamma_{\pi\pi}(k) + l_{ij}(\vec{k}) \bar{\Gamma}_{\pi\pi}(k) \right], \\ \Gamma_{A\pi ij}^{ab}(k) &= \delta^{ab} k_0 \left[\delta_{ij} \Gamma_{A\pi}(k) + l_{ij}(\vec{k}) \bar{\Gamma}_{A\pi}(k) \right] = \Gamma_{\pi A ij}^{ab}(-k), \\ \Gamma_{AA ij}^{ab}(k) &= i\delta^{ab} \vec{k}^2 \left[t_{ij}(\vec{k}) \Gamma_{AA}(k) + l_{ij}(\vec{k}) \bar{\Gamma}_{AA}(k) \right], \\ \Gamma_{\bar{q}q\alpha\beta}^{(0)}(k) &= i \left[\gamma^0 k_0 A_t(k) - \vec{\gamma} \cdot \vec{k} A_s(k) - B_m(k) + \gamma^0 k_0 \vec{\gamma} \cdot \vec{k} A_d(k) \right]_{\alpha\beta}\end{aligned}\quad (3.6)$$

where $l_{ij}(\vec{k}) = k_i k_j / \vec{k}^2$ is the longitudinal spatial projector and $t_{ij}(\vec{k}) = \delta_{ij} - l_{ij}(\vec{k})$ is the transverse spatial projector. All (scalar and dimensionless with the exception of B_m and A_d) dressing functions are functions of k_0^2 and \vec{k}^2 separately due to the inherent noncovariance of Coulomb gauge. At tree-level, the dressing functions reduce to (the tree-level forms for the proper two-point functions follow directly from the quadratic part of the action, \mathcal{S}^2 , given in Eq. (3.2))

$$\Gamma_{AA} = \Gamma_{A\pi} = \Gamma_{\pi\pi} = A_t = A_s = 1, \quad B_m = m, \quad \bar{\Gamma}_{AA} = \bar{\Gamma}_{A\pi} = \bar{\Gamma}_{\pi\pi} = A_d = 0. \quad (3.7)$$

Alongside the proper two-point functions, one is also interested in the corresponding propagators (connected two-point Green's functions). The connection between the connected and proper Green's functions is supplied via the Legendre transform. Since the components of the gluon field are treated individually in Coulomb gauge, the gluon propagator dressing function is not simply the inverse of the corresponding proper dressing function (as in Landau gauge) but rather, a matrix inversion structure arises. Taking into account the Lagrange multiplier fields that enforce the transversality of the \vec{A} and $\vec{\pi}$ -fields, the components of the gluon propagator are given by (see also Ref. [15])

$$\begin{aligned}W_{AA ij}^{ab}(k) &= i\delta^{ab} t_{ij}(\vec{k}) \frac{\Gamma_{\pi\pi}(k)}{\Delta_g(k)}, \\ W_{A\pi ij}^{ab}(k) &= -\delta^{ab} k_0 t_{ij}(\vec{k}) \frac{\Gamma_{A\pi}(k)}{\Delta_g(k)}, \\ W_{\pi\pi ij}^{ab}(k) &= i\delta^{ab} \vec{k}^2 t_{ij}(\vec{k}) \frac{\Gamma_{AA}(k)}{\Delta_g(k)}\end{aligned}\quad (3.8)$$

where the common denominator factor, $\Delta_g(k)$, including the Feynman prescription, is given by

$$\Delta_g(k) = k_0^2 \Gamma_{A\pi}^2(k) - \vec{k}^2 \Gamma_{AA}(k) \Gamma_{\pi\pi}(k) + i0_+. \quad (3.9)$$

In the case of the quarks (see Ref. [20]) we have

$$W_{\bar{q}q\alpha\beta}(k) = -\frac{i}{\Delta_f(k)} \left[\gamma^0 k_0 A_t(k) - \vec{\gamma} \cdot \vec{k} A_s(k) + B_m(k) + \gamma^0 k_0 \vec{\gamma} \cdot \vec{k} A_d(k) \right]_{\alpha\beta} \quad (3.10)$$

where the denominator factor is given by

$$\Delta_f(k) = k_0^2 A_t^2(k) - \vec{k}^2 A_s^2(k) - B_m^2(k) + k_0^2 \vec{k}^2 A_d^2(k) + i0_+. \quad (3.11)$$

The matrix inversion structure for the gluon and quark propagators will have important consequences when solving the Dyson-Schwinger equations. At tree-level, the denominator structures reduce to the familiar forms: $\Delta_g = k_0^2 - \vec{k}^2 + i0_+$ and $\Delta_f = k_0^2 - \vec{k}^2 - m^2 + i0_+$.

The tree-level vertex (three- and four-point proper) functions can be derived from the cubic and quartic parts of the action (\mathcal{S}^3 and \mathcal{S}^4 of Eq. (3.2), respectively). As for the two-point functions, the purely spatial tree-level vertex functions of the local first order formalism can be taken from Refs. [15, 20]. For these, the momentum space

expressions are

$$\begin{aligned}
\Gamma_{AAAijk}^{(0)abc}(k_1, k_2, k_3) &= -igf^{abc} [\delta_{ij}(k_1 - k_2)_k + \delta_{jk}(k_2 - k_3)_i + \delta_{ki}(k_3 - k_1)_j], \\
\Gamma_{AAAAijkl}^{(0)abcd}(k_1, k_2, k_3, k_4) &= -ig^2 [\delta_{ij}\delta_{kl}(f^{ace}f^{bde} - f^{ade}f^{bce}) + \delta_{ik}\delta_{jl}(f^{abe}f^{cde} - f^{ade}f^{bce}) \\
&\quad + \delta_{il}\delta_{jk}(f^{ace}f^{dbe} - f^{abe}f^{cde})], \\
\Gamma_{\bar{q}qA\alpha\beta i}^{(0)a}(k_1, k_2, k_3) &= -g [\gamma^i T^a]_{\alpha\beta},
\end{aligned} \tag{3.12}$$

where it is understood that all momenta are incoming and energy-momentum conservation has been applied ($\sum k_i = 0$). The new interaction terms that arise in the present nonlocal formalism, with the Ansatz that the Coulomb kernel be replaced by its expectation value, are all contained within the quartic component of the action (\mathcal{S}^4 of Eq. (3.2)). They are all linear in \tilde{F} and since the color charge ($\hat{\rho}$) involves both gluonic and quark components on the same footing, the tree-level vertices all have the same structure. It will be seen later that indeed, the resulting Dyson-Schwinger equations for the gluon and quark sectors have very similar forms. Using the techniques of Refs. [15, 20], the momentum space expressions for the vertices are:

$$\begin{aligned}
\Gamma_{AA\pi\pi ijkl}^{(0)abcd}(k_1, k_2, k_3, k_4) &= -ig^2 [f^{ead}f^{fbc}\delta_{il}\delta_{jk}\tilde{F}^{ef}(k_1 + k_4) + f^{ebd}f^{fac}\delta_{jl}\delta_{ik}\tilde{F}^{ef}(k_1 + k_3)], \\
\Gamma_{\bar{q}qA\pi\alpha\beta ij}^{(0)ab}(k_1, k_2, k_3, k_4) &= ig^2 f^{abe} [\gamma^0 T^f]_{\alpha\beta} \delta_{ij} \tilde{F}^{ef}(k_1 + k_2), \\
\Gamma_{\bar{q}q\bar{q}q\alpha\beta\gamma\delta}^{(0)}(k_1, k_2, k_3, k_4) &= -ig^2 [\gamma^0 T^a]_{\alpha\beta} [\gamma^0 T^b]_{\gamma\delta} \tilde{F}^{ab}(k_1 + k_2) + ig^2 [\gamma^0 T^a]_{\alpha\delta} [\gamma^0 T^b]_{\gamma\beta} \tilde{F}^{ba}(k_1 + k_4).
\end{aligned} \tag{3.13}$$

Notice that the above vertices are written such that the symmetry properties are manifest.

Let us now discuss the Dyson-Schwinger equations themselves. As stated earlier, we shall not present details of their derivation here: the basic techniques of such a derivation in Coulomb gauge are expounded in Refs. [15, 20]. Generically, the Dyson-Schwinger equations have a very definite structure of loop terms that arises from the combination of repeated functional differentiation of the generating functional and the Legendre transform connecting the connected and proper Green's functions. Once the notation and conventions have been established, different interaction terms merely follow this characteristic pattern; the difficulty is simply in keeping track of the various coefficients, especially where anticommuting Grassmann-valued fields (quarks or ghosts) are present.

The Dyson-Schwinger equations for the two-point proper functions (in momentum space) are presented below. To aid presentation, the two-loop terms that will not explicitly be used in this study are omitted (they are collectively denoted $\Gamma^{(2)}$ below). The equations are

$$\Gamma_{\pi\pi ij}^{ab}(k) = \Gamma_{\pi\pi ij}^{(0)ab}(k) - \frac{1}{2} \int \bar{d}\omega \Gamma_{AA\pi\pi kl ij}^{(0)c dab}(\omega, -\omega, k, -k) W_{AA lk}^{dc}(\omega) + \Gamma_{\pi\pi ij}^{(2)ab}(k), \tag{3.14}$$

$$\begin{aligned}
\Gamma_{\pi A ij}^{ab}(k) &= \Gamma_{\pi A ij}^{(0)ab}(k) - \int \bar{d}\omega \Gamma_{AA\pi\pi k j li}^{(0)cb da}(-\omega, -k, \omega, k) W_{A\pi kl}^{cd}(\omega) \\
&\quad + \int \bar{d}\omega \Gamma_{\bar{q}qA\pi\alpha\beta ji}^{(0)ba}(\omega, -\omega, -k, k) W_{\bar{q}q\beta\alpha}(\omega) + \Gamma_{\pi A ij}^{(2)ab}(k),
\end{aligned} \tag{3.15}$$

$$\begin{aligned}
\Gamma_{AA ij}^{ab}(k) &= \Gamma_{AA ij}^{(0)ab}(k) - \frac{1}{2} \int \bar{d}\omega \Gamma_{AA\pi\pi ij kl}^{(0)abcd}(k, -k, \omega, -\omega) W_{\pi\pi lk}^{dc}(\omega) - \frac{1}{2} \int \bar{d}\omega \Gamma_{AAAA ij kl}^{(0)abcd}(k, -k, \omega, -\omega) W_{AA lk}^{dc}(\omega) \\
&\quad + \frac{1}{2} \int \bar{d}\omega \Gamma_{AAA ikl}^{(0)acd}(k, -\omega, \omega - k) W_{AB k k'}^{cc'}(\omega) W_{AC l l'}^{dd'}(k - \omega) \Gamma_{CBA l' k' j}^{d'c'b}(k - \omega, \omega, -k) \\
&\quad - \int \bar{d}\omega \Gamma_{\bar{q}qA\alpha\beta i}^{(0)a}(\omega - k, -\omega, k) W_{\bar{q}q\beta\beta'}(\omega) \Gamma_{\bar{q}qA\beta'\alpha' j}^b(\omega, k - \omega, -k) W_{\bar{q}q\alpha'\alpha}(\omega - k) + \Gamma_{AA ij}^{(2)ab}(k),
\end{aligned} \tag{3.16}$$

$$\begin{aligned}
\Gamma_{\bar{q}q\alpha\beta}(k) &= \Gamma_{\bar{q}q\alpha\beta}^{(0)}(k) + \int \bar{d}\omega \Gamma_{\bar{q}q\bar{q}q\alpha\beta\gamma\delta}^{(0)}(k, -k, \omega, -\omega) W_{\bar{q}q\delta\gamma}(\omega) - \int \bar{d}\omega \Gamma_{\bar{q}qA\pi\alpha\beta kl}^{(0)cd}(k, -k, \omega, -\omega) W_{\pi Alk}^{dc}(\omega) \\
&\quad + \int \bar{d}\omega \Gamma_{\bar{q}qA\alpha\alpha' k}^{(0)c}(k, -\omega, \omega - k) W_{\bar{q}q\alpha'\beta'}(\omega) W_{AB k k'}^{cc'}(k - \omega) \Gamma_{\bar{q}qB\beta'\beta k'}^{c'}(\omega, -k, k - \omega) \\
&\quad + \Gamma_{\bar{q}q\alpha\beta}^{(2)}(k).
\end{aligned} \tag{3.17}$$

Because of the existence of the mixed gluon propagator $W_{A\pi}$ and the possibility of dressed vertices such as $\Gamma_{\pi\pi A}$ or $\Gamma_{\bar{q}q\pi}$, in certain terms of the above equations (in particular, the one-loop term of Eq. (3.16) involving the three-gluon vertex and the spatial one-loop component of the quark self-energy in the above) one must sum up over the possible

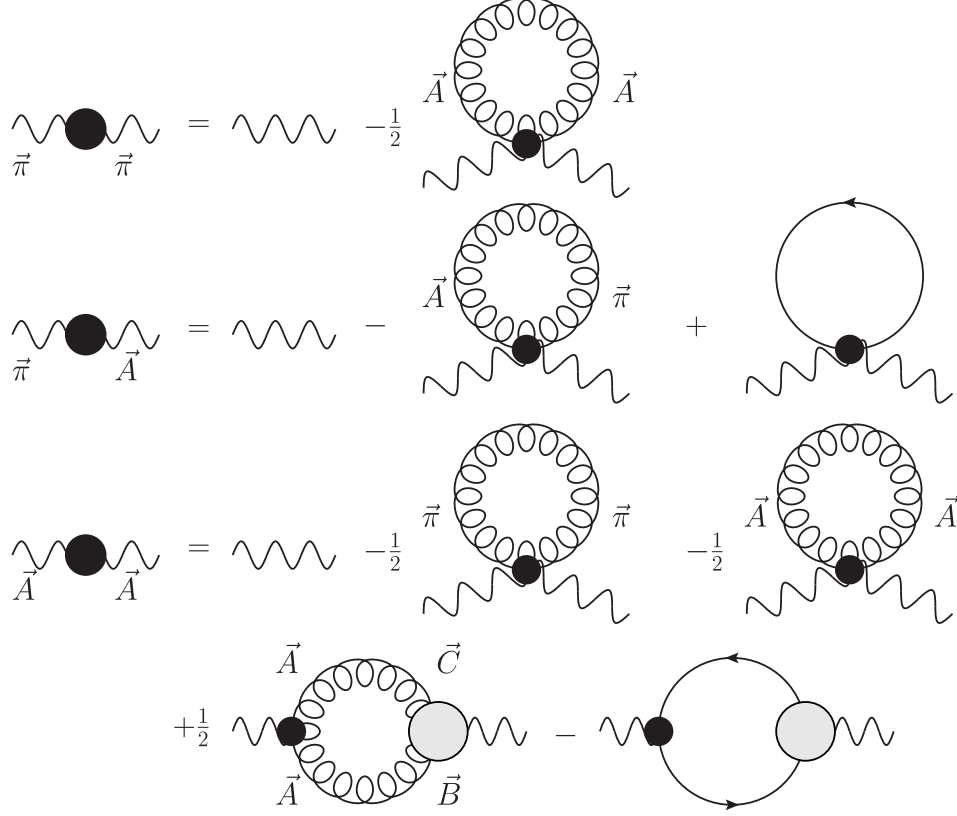


FIG. 1: Dyson-Schwinger equations for $\Gamma_{\pi\pi}$, $\Gamma_{\pi A}$ and Γ_{AA} , omitting two-loop terms. Wavy lines denote proper functions, the large filled blob indicating the dressed function. Springs denote gluonic propagators, lines denote the quark propagator and all internal propagators are dressed. Small blobs indicate tree-level vertices and large circles denote dressed vertices. The gluonic field types \vec{B} and \vec{C} denote the sum over \vec{A} and $\vec{\pi}$ contributions arising due to the presence of mixed gluon propagators. See text for details.

gluonic field types \vec{A} and $\vec{\pi}$: this sum is denoted by the repeated subscript indices \vec{B}, \vec{C}, \dots (obviously, no relation to the chromomagnetic or ghost fields). The equations are presented diagrammatically in Figs. 1 and 2. As mentioned previously, the Ansatz of replacing the Coulomb kernel with its expectation value in the action does not interfere with the one-loop Dyson-Schwinger equations. Inserting the appropriate tree-level vertices and propagators into the above equations and using

$$\tilde{F}^{ab}(k) = \delta^{ab} \frac{1}{\vec{k}^2} \quad (3.18)$$

(equivalent to the tree-level temporal gluon propagator), it can indeed be verified that the known one-loop perturbative expressions [18, 20] are recovered.

To complete this section, let us now describe the remainder of the truncation scheme. We are interested here in the leading loop, nonperturbative infrared behavior; in particular, on the effect of the terms generated directly by the Coulomb kernel, \tilde{F} . As discussed earlier, when replacing the full (nonlocal) Coulomb kernel with its expectation value within the action, one has already truncated out certain higher loop terms. The resulting Dyson-Schwinger equations retain their full leading (one-loop perturbative) structure. The next truncation we make on the Dyson-Schwinger equations is thus to restrict to the one-loop terms.

The next part of the truncation scheme is to omit those terms generated by the tree-level $\Gamma_{AAA}^{(0)}$, $\Gamma_{AAAA}^{(0)}$ and $\Gamma_{\bar{q}qA}^{(0)}$ vertices. These are the terms that are present at one-loop in the Dyson-Schwinger equations, but do not involve the Coulomb kernel directly. What remains of the Dyson-Schwinger equations are the tadpole terms involving the *tree-level* four-point vertices $\Gamma_{AA\pi\pi}^{(0)}$, $\Gamma_{\bar{q}qA\pi}^{(0)}$ and $\Gamma_{\bar{q}q\bar{q}q}^{(0)}$: these terms explicitly involve only the Coulomb kernel \tilde{F} and the propagators, thus forming a closed set of equations for a given input function \tilde{F} .

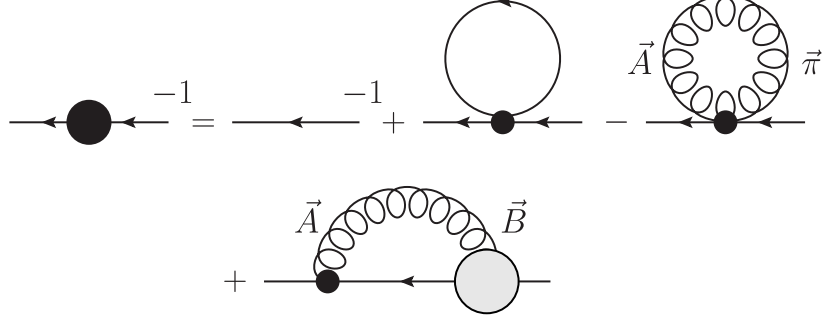


FIG. 2: Dyson-Schwinger equation for the quark two-point function, omitting two-loop terms. On the left-hand side, the filled blob indicates the dressed (inverse) propagator. Lines denote quark propagators, springs denote gluon propagators and all internal propagators are dressed. Small blobs indicate tree-level vertices and large circles denote dressed vertices. The gluonic field type \vec{B} represents the sum over \vec{A} and $\vec{\pi}$ contributions arising due to the presence of mixed gluon propagators. See text for details.

In order to complete the truncation scheme for the Dyson-Schwinger equations, we must supply an expression for the Coulomb kernel. This is based on an infrared divergent $1/\vec{k}^4$ behavior. In this study, we shall not include the perturbative ($1/\vec{k}^2$) term, since we are primarily interested in the infrared; however, an interesting point of note is that logarithmic ultraviolet divergences will still emerge (this will be discussed later). The $1/\vec{k}^4$ factor is justified on two grounds: lattice studies do show this behavior for the instantaneous component of the temporal gluon propagator, although the extant results admittedly do not go far enough into the infrared regime for this to be definitive [27–33]. The second reason is somewhat more pragmatic: as will be seen, such an infrared behavior is not only consistent with a linearly rising potential between heavy quarks but also generates dynamical chiral symmetry breaking for chiral quarks. Further, the product $g^2 \tilde{F}$ is a renormalization group invariant quantity [3, 26] and serves as an ideal quantity to use as input. For technical reasons, we use two forms for the input Coulomb kernel. The expressions are:

$$\begin{aligned}
 g^2 C_F \tilde{F}^{ab}(k) &= \delta^{ab} \mathcal{C} (2\pi)^3 \delta(\vec{k}) + \delta^{ab} F(\vec{k}^2), \\
 F(\vec{k}^2) &= 8\pi\sigma_c \begin{cases} \frac{1}{[\vec{k}^2]^2} & (\text{gluon/quark DSe}), \\ \frac{1}{[\vec{k}^2 + \xi]^2} & (\text{quark DSe}), \end{cases}
 \end{aligned} \tag{3.19}$$

where the coefficients have been chosen for later convenience ($C_F = (N_c^2 - 1)/2N_c$ is a color factor). The coefficient σ_c is the Coulomb string tension (as distinct from the physical Wilson string tension, see e.g., Refs. [33, 34] for a discussion). In the Dyson-Schwinger equations, an unadulterated $1/\vec{k}^4$ factor results in an infrared divergence, so that we will introduce a numerical infrared cutoff regulator. In the case of the quark, a second infrared mass regulator, ξ , will be considered — this form of regularization will turn out to have a very clear physical interpretation, which we will discuss later. Recall that the constant \mathcal{C} multiplying the δ -function (arising from the total charge constraint) is considered to be finite until the end of the calculation whereupon we consider the limit $\mathcal{C} \rightarrow \infty$.

IV. TRUNCATED DYSON-SCHWINGER EQUATIONS: ANALYTIC DEVELOPMENT

Let us now take the truncated Dyson-Schwinger equations and decompose them into a form useful for further analysis.

A. $\Gamma_{\pi A}$ equation

The truncated Dyson-Schwinger equation for $\Gamma_{\pi A}$, Eq. (3.15), reads

$$\begin{aligned}\Gamma_{\pi A ij}^{ab}(k) &= \Gamma_{\pi A ij}^{(0)ab}(k) - \int \bar{d}\omega \Gamma_{AA\pi\pi k j li}^{(0)cbda}(-\omega, -k, \omega, k) W_{A\pi kl}^{cd}(\omega) \\ &\quad + \int \bar{d}\omega \Gamma_{\bar{q}q A\pi\alpha\beta ji}^{(0)ba}(\omega, -\omega, -k, k) W_{\bar{q}q\beta\alpha}(\omega).\end{aligned}\quad (4.1)$$

Inserting the tree-level vertex functions using Eq. (3.13) and the general forms for the propagators and proper two-point function, Eqs. (3.8,3.6), one obtains

$$\begin{aligned}-\delta^{ab}k_0 \left[\delta_{ij}\Gamma_{A\pi}(k) + l_{ij}(\vec{k})\bar{\Gamma}_{A\pi}(k) \right] &= -\delta^{ab}k_0\delta_{ij} \\ -ig^2 \int \bar{d}\omega \left[f^{eca}f^{ebd}\delta_{ki}\delta_{jl}\tilde{F}(k-\omega) + f^{eba}f^{ecd}\delta_{ji}\delta_{kl}\tilde{F}(\omega-\omega) \right] &\delta^{cd}\omega_0 t_{kl}(\vec{\omega}) \frac{\Gamma_{A\pi}(\omega)}{\Delta_g(\omega)} \\ +g^2 f^{aeb} [\gamma^0 T^e]_{\alpha\beta} \delta_{ji} \int \frac{\bar{d}\omega}{\Delta_f(\omega)} \tilde{F}(\omega-\omega) &[\gamma^0\omega_0 A_t(\omega) - \vec{\gamma}\cdot\vec{\omega} A_s(\omega) + B_m(\omega) + \gamma^0\omega_0\vec{\gamma}\cdot\vec{\omega} A_d(\omega)]_{\beta\alpha}.\end{aligned}\quad (4.2)$$

We notice the occurrence of factors $\tilde{F}(\omega-\omega)$, which are technically undefined. However, the corresponding color structures read $f^{ecd}\delta^{cd}$ and $[T^e]_{\alpha\beta}\delta_{\beta\alpha}$, both of which are automatically zero. Assuming that \tilde{F} is infrared regulated, these terms would then pose no problem and we summarily dismiss them. Expanding the denominator factor Δ_g using Eq. (3.9), the equation then reads

$$\delta_{ij}\Gamma_{A\pi}(k) + l_{ij}(\vec{k})\bar{\Gamma}_{A\pi}(k) = \delta_{ij} - ig^2 N_c \int \frac{\bar{d}\omega \omega_0 \Gamma_{A\pi}(\omega)}{k_0 [\omega_0^2 \Gamma_{A\pi}^2(\omega) - \vec{\omega}^2 \Gamma_{AA}(\omega) \Gamma_{\pi\pi}(\omega) + i0_+]} t_{ij}(\vec{\omega}) \tilde{F}(k-\omega). \quad (4.3)$$

Since \tilde{F} is independent of the energy and the scalar dressing functions Γ_{AA} , $\Gamma_{A\pi}$, $\Gamma_{\pi\pi}$ are all even functions of energy, the integrand is overall odd in the energy and thus vanishes without further assumption. We thus have the nonperturbative result that under the current truncation scheme,

$$\Gamma_{A\pi}(k) = 1, \quad \bar{\Gamma}_{A\pi}(k) = 0. \quad (4.4)$$

In other words, the mixed gluon two-point proper function remains bare. This result is very useful because as will be seen below, the energy dependence of the gluon propagators turns out to be trivial.

B. $\Gamma_{\pi\pi}$ and Γ_{AA} : the gluon gap equation

The truncated Dyson-Schwinger equations for $\Gamma_{\pi\pi}$ and Γ_{AA} , Eqs. (3.14,3.16), can be treated simultaneously. They read

$$\begin{aligned}\Gamma_{\pi\pi ij}^{ab}(k) &= \Gamma_{\pi\pi ij}^{(0)ab}(k) - \frac{1}{2} \int \bar{d}\omega \Gamma_{AA\pi\pi k l ij}^{(0)cdab}(\omega, -\omega, k, -k) W_{AA lk}^{dc}(\omega), \\ \Gamma_{AA ij}^{ab}(k) &= \Gamma_{AA ij}^{(0)ab}(k) - \frac{1}{2} \int \bar{d}\omega \Gamma_{AA\pi\pi ij kl}^{(0)abcd}(k, -k, \omega, -\omega) W_{\pi\pi lk}^{dc}(\omega).\end{aligned}\quad (4.5)$$

Notice that having restricted the truncation scheme to include only those one-loop terms involving the Coulomb kernel, the two equations are identical in their structure. Inserting the tree-level vertex functions, Eq. (3.13), the two-point function decompositions, Eqs. (3.6,3.8,3.9), projecting onto the transverse components (the longitudinal components of the proper two-point functions will play no role) and using the previous result that $\Gamma_{A\pi} = 1$ within this truncation scheme, one readily obtains

$$\begin{aligned}\Gamma_{\pi\pi}(k) &= 1 + \frac{i}{2} g^2 N_c \int \frac{\bar{d}\omega \Gamma_{\pi\pi}(\omega)}{[\omega_0^2 - \vec{\omega}^2 \Gamma_{AA}(\omega) \Gamma_{\pi\pi}(\omega) + i0_+]} \tilde{F}(k-\omega) t_{ji}(\vec{k}) t_{ij}(\vec{\omega}), \\ \Gamma_{AA}(k) &= 1 + \frac{i}{2} g^2 N_c \int \frac{\bar{d}\omega \vec{\omega}^2 \Gamma_{AA}(\omega)}{\vec{k}^2 [\omega_0^2 - \vec{\omega}^2 \Gamma_{AA}(\omega) \Gamma_{\pi\pi}(\omega) + i0_+]} \tilde{F}(k-\omega) t_{ji}(\vec{k}) t_{ij}(\vec{\omega}).\end{aligned}\quad (4.6)$$

Given that \tilde{F} is energy independent, the energy integrals of the above are relatively trivial and since there is no k_0 -dependence, the proper dressing functions are energy independent. However, we should point out that really, the energy integral is only trivial if the spatial functions are regularized and finite. Here, this refers to an implicit infrared regularization in the case of $\tilde{F} \sim 1/\vec{k}^4$ with its strong infrared singularity, the finite coefficient \mathcal{C} multiplying $\delta(\vec{k})$ and more generally, the ultraviolet cutoff when one considers the perturbative term $\tilde{F} \sim 1/\vec{k}^2$ although we shall see that the Γ_{AA} equation involves a logarithmic UV divergence even with the $1/\vec{k}^4$ interaction. It is helpful to define the static propagators $W^{(s)}$ as the energy integral of the full propagators (in configuration space, these are the equaltime propagators). In the case of the W_{AA} propagator,

$$W_{AAij}^{(s)ab}(\vec{k}) = i\delta^{ab}t_{ij}(\vec{k}) \int_{-\infty}^{\infty} \frac{dk_0}{2\pi} \frac{\Gamma_{\pi\pi}(\vec{k}^2)}{[k_0^2 - \vec{k}^2\Gamma_{AA}(\vec{k}^2)\Gamma_{\pi\pi}(\vec{k}^2) + i0_+]} = \delta^{ab}t_{ij}(\vec{k}) \int_{-\infty}^{\infty} \frac{dk_4}{2\pi} \frac{\Gamma_{\pi\pi}(\vec{k}^2)}{[k_4^2 + \vec{k}^2\Gamma_{AA}(\vec{k}^2)\Gamma_{\pi\pi}(\vec{k}^2)]} \quad (4.7)$$

where in the second integral form, a Wick rotation ($k_0 \rightarrow ik_4$) has been performed. Doing the integral, one finds that the static propagator $W_{AA}^{(s)}$ can be written in terms of a single dressing function, which we denote G :

$$W_{AAij}^{(s)ab}(\vec{k}) = \delta^{ab}t_{ij}(\vec{k}) \frac{1}{2|\vec{k}|} G(\vec{k}^2)^{1/2}, \quad G(\vec{k}^2) = \frac{\Gamma_{\pi\pi}(\vec{k}^2)}{\Gamma_{AA}(\vec{k}^2)}. \quad (4.8)$$

The static propagator $W_{\pi\pi}^{(s)}$ can also be written in terms of G :

$$W_{\pi\pi ij}^{(s)ab}(\vec{k}) = \delta^{ab}t_{ij}(\vec{k}) \frac{|\vec{k}|}{2} G(\vec{k}^2)^{-1/2}. \quad (4.9)$$

The reduction of the two dressing functions Γ_{AA} and $\Gamma_{\pi\pi}$ to a single function G follows directly from the previous result $\Gamma_{A\pi} = 1$.

Returning to the Dyson-Schwinger equations, we can now write

$$\begin{aligned} \Gamma_{\pi\pi}(\vec{k}^2) &= 1 + \frac{1}{4}g^2 N_c \int \frac{d\vec{\omega}}{\sqrt{\vec{\omega}^2}} G(\vec{\omega}^2)^{1/2} \tilde{F}(k - \omega) t_{ji}(\vec{k}) t_{ij}(\vec{\omega}), \\ \Gamma_{AA}(\vec{k}^2) &= 1 + \frac{1}{4}g^2 N_c \int \frac{d\vec{\omega}}{\sqrt{\vec{\omega}^2}} \frac{\vec{\omega}^2}{\vec{k}^2} G(\vec{\omega}^2)^{-1/2} \tilde{F}(k - \omega) t_{ji}(\vec{k}) t_{ij}(\vec{\omega}) \end{aligned} \quad (4.10)$$

where $d\vec{\omega} = d\vec{\omega}/(2\pi)^3$. Expanding out \tilde{F} with Eq. (3.19) we have

$$\begin{aligned} \Gamma_{\pi\pi}(\vec{k}^2) &= 1 + \frac{1}{2} \frac{N_c}{C_F} \frac{\mathcal{C}}{\sqrt{\vec{k}^2}} G(\vec{k}^2)^{1/2} + \frac{1}{4} \frac{N_c}{C_F} \int \frac{d\vec{\omega}}{\sqrt{\vec{\omega}^2}} G(\vec{\omega}^2)^{1/2} F(\vec{k} - \vec{\omega}) t_{ji}(\vec{k}) t_{ij}(\vec{\omega}), \\ \Gamma_{AA}(\vec{k}^2) &= 1 + \frac{1}{2} \frac{N_c}{C_F} \frac{\mathcal{C}}{\sqrt{\vec{k}^2}} G(\vec{k}^2)^{-1/2} + \frac{1}{4} \frac{N_c}{C_F} \int \frac{d\vec{\omega}}{\sqrt{\vec{\omega}^2}} \frac{\vec{\omega}^2}{\vec{k}^2} G(\vec{\omega}^2)^{-1/2} F(\vec{k} - \vec{\omega}) t_{ji}(\vec{k}) t_{ij}(\vec{\omega}). \end{aligned} \quad (4.11)$$

The proper dressing functions, $\Gamma_{\pi\pi}$ and Γ_{AA} (and subsequently, the corresponding propagators), are explicitly dependent not only on \mathcal{C} , but also include potentially infrared divergent contributions stemming from the integrals involving F . However, using the definition of G , one can easily see that the above equations can be written in terms of a single equation for G :

$$G(\vec{k}^2) = 1 + \frac{1}{4} \frac{N_c}{C_F} \int \frac{d\vec{\omega}}{\sqrt{\vec{\omega}^2}} F(\vec{k} - \vec{\omega}) t_{ji}(\vec{k}) t_{ij}(\vec{\omega}) \left[G(\vec{\omega}^2)^{1/2} - \frac{\vec{\omega}^2}{\vec{k}^2} \frac{G(\vec{k}^2)}{G(\vec{\omega}^2)^{1/2}} \right]. \quad (4.12)$$

The terms proportional to \mathcal{C} cancel, showing that G and the static propagators are independent of \mathcal{C} . In addition, one sees that the infrared divergence of F is tempered, such that G may be infrared finite (as will be seen). It would thus appear that the physical dynamics are contained within the static propagator dressing function, whereas the full propagators (and in particular, their pole positions) are not physical. We shall discuss this at the end. For reasons that will become obvious shortly, we shall refer to Eq. (4.12) as the gluon gap equation. The form of the equation is identical to that for the static gluon propagator derived from the canonical approach [6] (see also the earlier work of Refs. [4, 13]). In the canonical approach, the Coulomb kernel F (here an input) is represented by a combination of ghost dressing and Coulomb form factors, which are self-consistently determined from their respective equations. Later work within the canonical approach included further terms: the ghost ‘curvature’ [7–9], and three- and four-gluon interactions [10]. The equivalence of the truncated Dyson-Schwinger equation above, Eq. (4.12), to its counterpart arising from the canonical formalism and considered in Ref. [6] is one of the results of this paper.

C. $\Gamma_{\bar{q}q}$: the quark gap equation

Under truncation, the Dyson-Schwinger equation for $\Gamma_{\bar{q}q}$, Eq. (3.17), reads

$$\Gamma_{\bar{q}q\alpha\beta}(k) = \Gamma_{\bar{q}q\alpha\beta}^{(0)}(k) + \int \bar{d}\omega \Gamma_{\bar{q}q\alpha\beta\gamma\delta}^{(0)}(k, -k, \omega, -\omega) W_{\bar{q}q\delta\gamma}(\omega) - \int \bar{d}\omega \Gamma_{\bar{q}qA\pi\alpha\beta kl}^{(0)cd}(k, -k, \omega, -\omega) W_{\pi Alk}^{dc}(\omega). \quad (4.13)$$

Inserting the appropriate tree-level vertices, Eq. (3.13) and propagators, Eqs. (3.8,3.10), resolving the color algebra (again discarding terms where one has $\text{Tr}[T^a]$ or f^{cac} that multiply $\tilde{F}(\omega - \omega)$ as previously discussed for $\Gamma_{A\pi}$), one obtains

$$\Gamma_{\bar{q}q\alpha\beta}(k) = \Gamma_{\bar{q}q\alpha\beta}^{(0)}(k) + g^2 C_F \int \frac{\bar{d}\omega \tilde{F}(k - \omega)}{\Delta_f(\omega)} [\gamma^0 \omega_0 A_t(\omega) - \gamma^0 \vec{\gamma} \cdot \vec{\omega} \gamma^0 A_s(\omega) + B_m + \vec{\gamma} \cdot \vec{\omega} \gamma^0 \omega_0 A_d(\omega)]_{\alpha\beta}, \quad (4.14)$$

where it is again recognized that \tilde{F} is independent of the energy. Projecting out the Dirac components in the decomposition for $\Gamma_{\bar{q}q}$, Eq. (3.6), one obtains four equations for the dressing functions:

$$A_t(k) = 1 - ig^2 C_F \int \frac{\bar{d}\omega \omega_0 A_t(\omega) \tilde{F}(k - \omega)}{k_0 \Delta_f(\omega)}, \quad (4.15)$$

$$A_s(k) = 1 + ig^2 C_F \int \frac{\bar{d}\omega \vec{k} \cdot \vec{\omega} A_s(\omega) \tilde{F}(k - \omega)}{\vec{k}^2 \Delta_f(\omega)}, \quad (4.16)$$

$$B_m(k) = m + ig^2 C_F \int \frac{\bar{d}\omega B_m(\omega) \tilde{F}(k - \omega)}{\Delta_f(\omega)}, \quad (4.17)$$

$$A_d(k) = ig^2 C_F \int \frac{\bar{d}\omega \omega_0 \vec{k} \cdot \vec{\omega} A_d(\omega) \tilde{F}(k - \omega)}{k_0 \vec{k}^2 \Delta_f(\omega)}. \quad (4.18)$$

As for the $\Gamma_{A\pi}$ equation, the odd energy integrals vanish since all dressing functions are functions of ω_0^2 (including Δ_f), furnishing the result that

$$A_t(k) = 1, \quad A_d(k) = 0. \quad (4.19)$$

In addition, one sees that A_s and B_m are independent of energy. The static quark propagator, defined in analogy to the gluon propagator, is then

$$W_{\bar{q}q\alpha\beta}^{(s)}(\vec{k}) = -i \int_{-\infty}^{\infty} \frac{dk_0}{2\pi} \frac{[\gamma^0 k_0 - \vec{\gamma} \cdot \vec{k} A_s(\vec{k}^2) + B_m(\vec{k}^2)]_{\alpha\beta}}{[k_0^2 - \vec{k}^2 A_s^2(\vec{k}^2) - B_m^2(\vec{k}^2) + i0_+]} = \int_{-\infty}^{\infty} \frac{dk_4}{2\pi} \frac{[\vec{\gamma} \cdot \vec{k} A_s(\vec{k}^2) - B_m(\vec{k}^2)]_{\alpha\beta}}{[k_4^2 + \vec{k}^2 A_s^2(\vec{k}^2) + B_m^2(\vec{k}^2)]} \quad (4.20)$$

and performing the integral, one obtains

$$W_{\bar{q}q\alpha\beta}^{(s)}(\vec{k}) = \frac{[\vec{\gamma} \cdot \vec{k} - M(\vec{k}^2)]_{\alpha\beta}}{2\sqrt{\vec{k}^2 + M(\vec{k}^2)^2}}, \quad M(\vec{k}^2) = \frac{B_m(\vec{k}^2)}{A_s(\vec{k}^2)}. \quad (4.21)$$

The static quark propagator can thus be written in terms of a single mass function, M . This is analogous to the case for the static gluon propagator. Expanding \tilde{F} with Eq. (3.19), the equations for A_s and B_m can be written as

$$\begin{aligned} A_s(\vec{k}^2) &= 1 + \frac{1}{2} \frac{\mathcal{C}}{\sqrt{\vec{k}^2 + M(\vec{k}^2)^2}} + \frac{1}{2} \int \frac{\bar{d}\vec{\omega} \vec{k} \cdot \vec{\omega} F(\vec{k} - \vec{\omega})}{\vec{k}^2 \sqrt{\vec{\omega}^2 + M(\vec{\omega}^2)^2}}, \\ B_m(\vec{k}^2) &= m + \frac{1}{2} \frac{\mathcal{C} M(\vec{k}^2)}{\sqrt{\vec{k}^2 + M(\vec{k}^2)^2}} + \frac{1}{2} \int \frac{\bar{d}\vec{\omega} M(\vec{\omega}^2) F(\vec{k} - \vec{\omega})}{\sqrt{\vec{\omega}^2 + M(\vec{\omega}^2)^2}}. \end{aligned} \quad (4.22)$$

Clearly the functions A_s , B_m (and hence the full quark propagator) are dependent on \mathcal{C} and involve potentially infrared divergent integrals, just as for the gluon. Combining the above equations, we see that the \mathcal{C} -dependence of M cancels:

$$M(\vec{k}^2) = m + \frac{1}{2} \int \frac{\bar{d}\vec{\omega} F(\vec{k} - \vec{\omega})}{\sqrt{\vec{\omega}^2 + M(\vec{\omega}^2)^2}} \left[M(\vec{\omega}^2) - \frac{\vec{k} \cdot \vec{\omega}}{\vec{k}^2} M(\vec{k}^2) \right] \quad (4.23)$$

and one again sees that although F may be strongly infrared divergent, M can still be infrared finite. Equation (4.23) is the quark gap equation and moreover, is well-known from the literature as the Adler-Davis truncation [12], where it was derived using the canonical Hamiltonian approach. A more advanced version of the quark gap equation to self-consistently include the spatial quark gluon vertex has been recently studied in the canonical approach [11]. The equivalence of Eq. (4.23) to the previously derived gap equation for the static propagator in the canonical approach [12] is again a result of this study. The similarity of the quark gap equation, Eq. (4.23), to its gluonic counterpart, Eq. (4.12), is striking (and this is why we take the liberty in referring to Eq. (4.12) as the gluon gap equation) and arises primarily from the truncation to include only those terms originating from the Coulomb kernel, which itself involves both the quark and gluon contributions to the color charge on equal footing.

It is possible to make a connection between the (full) quark propagator and the leading order heavy quark propagator in Coulomb gauge [23] (see also [24, 25]). This is based on a spin-decomposition and we follow the spirit of Ref. [35]. Let us introduce the spin-projection operators

$$P_{\pm} = \frac{1}{2} (\mathbb{1} \pm \gamma^0), \quad P_+ + P_- = \mathbb{1}, \quad P_+ P_- = 0, \quad P_{\pm}^2 = P_{\pm}. \quad (4.24)$$

These projectors furnish the following identities:

$$P_+ \gamma^0 P_+ = P_+ P_+, \quad P_- \gamma^0 P_- = -P_- P_-, \quad P_+ \gamma^0 P_- = P_+ \gamma^i P_+ = P_- \gamma^i P_- = 0 \quad (4.25)$$

which allow us to write the quark propagator as

$$\begin{aligned} W_{\bar{q}q\alpha\beta}(k) &= [(P_+ + P_-) W_{\bar{q}q}(k) (P_+ + P_-)]_{\alpha\beta} \\ &= \frac{(-i)}{\left[k_0^2 - \vec{k}^2 A_s^2(\vec{k}^2) - B_m^2(\vec{k}^2) + i0_+ \right]} \\ &\quad \times \left\{ \left[k_0 + B_m(\vec{k}^2) \right] P_+ P_+ - \left[k_0 - B_m(\vec{k}^2) \right] P_- P_- - \left[P_+ \vec{\gamma} \cdot \vec{k} P_- + P_- \vec{\gamma} \cdot \vec{k} P_+ \right] A_s(\vec{k}^2) \right\}_{\alpha\beta}. \end{aligned} \quad (4.26)$$

The heavy quark limit for Coulomb gauge (implicitly in the rest frame) can be expressed as the limit $|\vec{k}|/m \rightarrow 0$. Considering Eq. (4.23), we can make a leading order estimate for the function M (and we shall see that this is confirmed by the numerical results). Given that $F(\vec{k} - \vec{\omega})$ in the integral peaks at $\vec{\omega} = \vec{k}$, the infrared divergence is canceled and leaves

$$M(\vec{k}^2) \approx m + \# \frac{M(\vec{k}^2)}{\sqrt{\vec{k}^2 + M^2(\vec{k}^2)}} \xrightarrow{|\vec{k}| \ll m} m + \#. \quad (4.27)$$

The functions A_s , B_m given by Eq. (4.22) can also then be estimated:

$$\begin{aligned} A_s(\vec{k}^2) &\xrightarrow{|\vec{k}| \ll m} 1 + \mathcal{O}(1/m) \\ B_m(\vec{k}^2) &\xrightarrow{|\vec{k}| \ll m} m + \frac{1}{2}\mathcal{C} + \frac{1}{2} \int d\vec{\omega} F(\vec{\omega}^2) \quad (= B_m) \end{aligned} \quad (4.28)$$

where in B_m , it is recognized that the integral is infrared divergent and not suppressed by factors $1/m$. We demand that $|\vec{k}|A_s \rightarrow 0$, despite the fact that $\mathcal{C} \rightarrow \infty$ (in the heavy quark limit, m is the largest scale). The spin-decomposed quark propagator in the heavy quark limit is then

$$\begin{aligned} W_{\bar{q}q\alpha\beta}(k) &\xrightarrow{|\vec{k}| \ll m} \frac{(-i)}{[k_0^2 - B_m^2 + i0_+]} \{ [k_0 + B_m] P_+ P_+ - [k_0 - B_m] P_- P_- \}_{\alpha\beta} \\ &= -i \frac{[P_+ P_+]_{\alpha\beta}}{[k_0 - B_m + i\varepsilon]} + i \frac{[P_- P_-]_{\alpha\beta}}{[k_0 + B_m - i\varepsilon]}. \end{aligned} \quad (4.29)$$

The first component represents a heavy quark propagating forward in time; the second, a heavy antiquark propagating backwards in time (and under time-reversal is equivalent to the first component). The first component is explicitly that found in Ref. [23] (and where only forward propagation is included), showing that the leading loop order Dyson-Schwinger truncation scheme considered here reduces in the heavy quark limit to the scheme considered previously. Notice that when considering the heavy quark limit for the Bethe-Salpeter equation [23], the Faddeev equation [24] and the quark four-point Dyson-Schwinger equation [25], the constant \mathcal{C} and the infrared divergence of the spatial integral over F that occur in B_m , Eq. (4.28), cancel explicitly when considering color singlet quark configurations.

V. TRUNCATED DYSON-SCHWINGER EQUATIONS: NUMERICAL ANALYSIS

Let us now consider the numerical solutions to the gap equations (4.12,4.23) for the static dressing functions G and M . The defining feature of the truncated gap equations is the input Coulomb kernel $F \sim 1/\vec{k}^4$. The strong singularity is also the defining problem in solving the equations.

A. gluon gap equation

In order to solve the gluon gap equation, Eq. (4.12), it proves convenient to change integration variables such that the radial integration momentum goes through the Coulomb kernel. The equation thus reads (to make the equation more readable, we use subscripts to denote the momentum dependence of the functions)

$$G_k = 1 + \frac{N_c}{4C_F} \int \frac{d\vec{\omega}}{\sqrt{(\vec{k} - \vec{\omega})^2}} F_{\omega} t_{ji}(\vec{k}) t_{ij}(\vec{k} - \vec{\omega}) \left[G_{k-\omega}^{1/2} - \frac{(\vec{k} - \vec{\omega})^2}{\vec{k}^2} \frac{G_k}{G_{k-\omega}^{1/2}} \right]. \quad (5.1)$$

The above equation is not renormalized nor is it regularized. It is convenient to use the following notation:

$$x = \vec{k}^2, \quad y = \vec{\omega}^2, \quad \theta = (\vec{k} - \vec{\omega})^2 = x + y - 2\sqrt{xy}z, \quad \int d\vec{\omega} \rightarrow \frac{2}{(4\pi)^2} \int_{\varepsilon}^{\Lambda} dy \sqrt{y} \int_{-1}^1 dz \quad (5.2)$$

where both an ultraviolet (UV), $\Lambda \rightarrow \infty$, and an infrared (IR), $\varepsilon \rightarrow 0$, spatial momentum cutoff have been introduced to regularize the integrals. Inserting the first form of Eq. (3.19) for F , the equation reads

$$G_x = 1 + \sigma_c \gamma \int_{\varepsilon}^{\Lambda} \frac{dy}{y} \int_{-1}^1 \frac{dz}{\sqrt{y\theta}} K(x, y; z) \left[G_{\theta}^{1/2} - \frac{\theta}{x} \frac{G_x}{G_{\theta}^{1/2}} \right], \quad (5.3)$$

where

$$\gamma = \frac{N_c^2}{\pi(N_c^2 - 1)}, \quad K(x, y; z) = 1 - \frac{y(1 - z^2)}{2\theta}. \quad (5.4)$$

One immediately sees the effect of the strong IR singularity present in the kernel: as $y \rightarrow 0$, there must exist some cancellation such that the solution is independent of the IR-cutoff (ε). In effect, the combination of terms in the last bracket must cancel to leading order in y , such that the angular integral vanishes as $y \rightarrow 0$ (and for all values of x). Let us therefore consider the angular integral in some more detail:

$$I_z(x, y) = \int_{-1}^1 \frac{dz}{\sqrt{y\theta}} K(x, y; z) \left[G_{\theta}^{1/2} - \frac{\theta}{x} \frac{G_x}{G_{\theta}^{1/2}} \right]. \quad (5.5)$$

For large values of x and vanishing y , $\theta = x + \mathcal{O}(y)$ and $G_{\theta} \rightarrow G_x + \mathcal{O}(y)$. Then, it is obvious that

$$I_z(x, y) \sim \int_{-1}^1 \frac{dz}{\sqrt{yx}} \left[1 - \frac{y(1 - z^2)}{2x} \right] \left[G_x^{1/2} \mathcal{O}(y) \right] \quad (5.6)$$

which would then automatically lead to an overall IR convergent radial integral. The case where both x and y are small is slightly more complicated. In the process of regularization, an additional (mass) scale is introduced so let us assume that to leading order in the IR,

$$G_x \xrightarrow{x \rightarrow 0} G_0 \left(\frac{x}{\kappa_0} \right)^{\alpha}, \quad (5.7)$$

where κ_0 has dimension $[mass]^2$ and G_0 is some constant. The angular integral would then read

$$I_z(x, y) = G_0^{1/2} \int_{-1}^1 \frac{dz}{\sqrt{y\theta}} K(x, y; z) \left(\frac{\theta}{\kappa_0} \right)^{\alpha/2} \left[1 - \left(\frac{x}{\theta} \right)^{\alpha-1} + \mathcal{O}(y) \right] \quad (5.8)$$

which can only have the necessary cancellation (given that x may be of the same order as y , but is still unfixed) for $\alpha = 1$. Thus, the cancellation of the IR singularity leads us to consider a solution of the form

$$G_x = \frac{x}{x + \kappa_x} \quad (5.9)$$

where for low x , κ_x should be a constant. Indeed, in Ref. [6] where the gluon gap equation was solved with an infrared enhanced (but not $1/\vec{k}^4$) Coulomb kernel, such a solution with a constant κ_x was shown to be a good approximation to the full solution. Note that for such a solution, the static gluon propagator ($\sim G_x^{1/2}/\sqrt{x}$) has a constant asymptotic value in the IR, characteristic of a massive solution and contradicting the analysis of [36] (see also, Ref. [37]), i.e., the propagator does not have the Gribov form [1].

The gluon gap equation, Eq. (5.3) can be recast as an equation for κ_x :

$$\kappa_x = \sigma_c \gamma \int_{\varepsilon}^{\Lambda} \frac{dy}{y} \int_{-1}^1 dz K(x, y; z) \frac{[\theta - x + \kappa_{\theta} - \kappa_x]}{\sqrt{y}\sqrt{\theta + \kappa_{\theta}}}. \quad (5.10)$$

Let us discuss the UV behavior of κ_x . Assuming that for finite, but large x , $x \gg \kappa_x$, then

$$\kappa_x \approx \sigma_c \gamma \int_{\varepsilon}^{\Lambda} \frac{dy}{y} \int_{-1}^1 dz K(x, y; z) \frac{[\theta - x]}{\sqrt{y}\sqrt{\theta}}. \quad (5.11)$$

For $y \gg x$ (the upper limit of the radial integral), we would then have

$$\kappa_x \sim \sigma_c \gamma \int_{\varepsilon}^{\Lambda} \frac{dy}{y} \int_{-1}^1 dz \frac{1}{2} (1 + z^2) \sim \frac{4}{3} \sigma_c \gamma \ln(\Lambda) \quad (5.12)$$

which after balancing dimensions leads us to the leading UV behavior for κ_x :

$$\kappa_x \sim -\frac{4}{3} \sigma_c \gamma \ln\left(\frac{x}{\Lambda}\right). \quad (5.13)$$

Thus, although there is no perturbative content in the Coulomb kernel ($\sim 1/\vec{k}^4$), there is still a logarithmic UV-divergent contribution to the static gluon propagator. Moreover, the factor $4/3$, arising from the angular integral is characteristic to the ghost self-energy (see e.g., Ref. [38]). It appears rather ironic that the function κ_x , which was introduced to cancel the leading IR singularity, is connected to the UV-cutoff, but in retrospect this is quite natural: the IR scale appears during regularization (breaking the scale invariance of the original theory). Further, the divergent term originates in the Γ_{AA} -equation which, were one to have the perturbative form for F ($\sim 1/\vec{k}^2$), gives rise to a quadratic UV-divergence that is canceled by the gluon loop. Here, the quadratic divergence is reduced to a logarithmic divergence. One sees therefore that in Coulomb gauge, the nonperturbative UV-limit is not necessarily the same thing as the perturbative limit.

Equation (5.10) is solved by iteration, to give the unrenormalized function κ_x in terms of the UV-cutoff Λ . In order to numerically cope with the infrared divergence, the equation is rewritten in the form

$$\kappa_x(\Lambda) = \frac{I_1(x; \varepsilon, \Lambda)}{1 + I_2(x; \varepsilon, \Lambda)} \quad (5.14)$$

where

$$\begin{aligned} I_1(x; \varepsilon, \Lambda) &= \sigma_c \gamma \int_{\varepsilon}^{\Lambda} \frac{dy}{y} \int_{-1}^1 dz K(x, y; z) \frac{[\theta - x + \kappa_{\theta}]}{\sqrt{y}\sqrt{\theta + \kappa_{\theta}}}, \\ I_2(x; \varepsilon, \Lambda) &= \sigma_c \gamma \int_{\varepsilon}^{\Lambda} \frac{dy}{y} \int_{-1}^1 dz K(x, y; z) \frac{1}{\sqrt{y}\sqrt{\theta + \kappa_{\theta}}}. \end{aligned} \quad (5.15)$$

The reason for using this form is that during iteration, where κ within the integral is not yet the solution, the infrared cancellation required for Eq. (5.10) may not happen in practice and the error is amplified by the latent infrared singularity: the iteration procedure would thus be unstable. Both I_1 and I_2 diverge as $\varepsilon \rightarrow 0$ (the divergence is $\sim 1/\sqrt{\varepsilon}$ in both cases) such that numerically their difference will be inherently prone to a loss of fidelity and the residues of the singularities are not known exactly enough to compensate. The ratio of the two integrals is better behaved such that with the form Eq. (5.14), the iteration is stable (but only slowly convergent). In the end, both forms of the equation are satisfied.

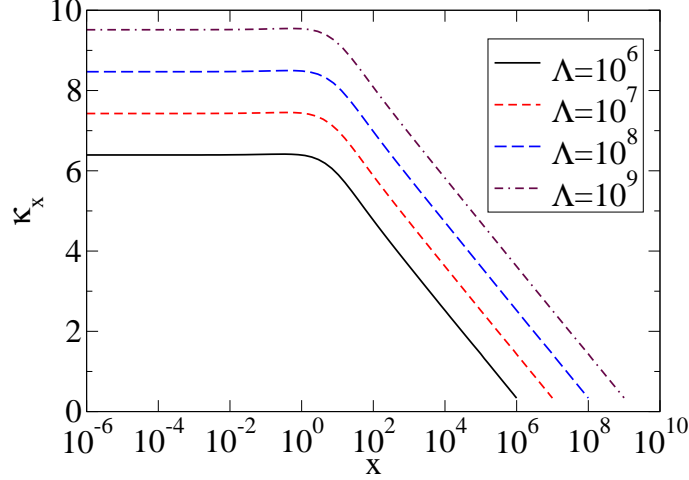


FIG. 3: Plot of κ_x for various values of the UV-cutoff, Λ . All dimensionful quantities are in units of σ_c . See text for details.

Λ	a_0	\bar{a}_0	b_1
10^6	6.39	6.37	-0.475
10^7	7.43	7.40	-0.475
10^8	8.47	8.44	-0.474
10^9	9.51	9.48	-0.474

TABLE I: Numerical values for fitted coefficients for various values of Λ . All dimensionful quantities are in units of σ_c . See text for details.

As input, we take the values $N_c = 3$ and $\sigma_c = 1$ (all dimensionful quantities are thus expressed in units of σ_c for now). The radial and angular integrals are performed using (standard) Gaussian quadrature grids. In the integrand, κ_θ is evaluated using either cubic spline interpolation derived from the grid of x -values or, for asymptotic arguments, extrapolation based on the following formulae:

$$\kappa_x = \begin{cases} a_0 + a_1 x + a_2 x^2, & \text{small } x \\ b_0 + b_1 \ln(x), & \text{large } x \end{cases}. \quad (5.16)$$

In practice, the fit to the UV asymptotic form is performed for $x \in [\Lambda/10^3, \Lambda/10]$ in order to avoid complications arising when $x \sim \Lambda$. It is found that for $\varepsilon \leq 10^{-6}$, κ_x becomes independent of ε , as it should. κ_x is plotted in Fig. 3 for various values of Λ . It is seen that in the IR, κ_x goes to a constant value, whereas in the UV, it decreases logarithmically, confirming the previous analysis. The extracted values for the asymptotic coefficients a_0 (the infrared constant value of κ_x) and b_1 (the slope of the UV-logarithmic divergence) are given in Table I. The analytic value for b_1 according to Eq. (5.13) is -0.477 with the current input and one sees that this is numerically verified (to within a reasonable numerical precision of $< 1\%$, recalling that the integrals themselves involve $\mathcal{O}(1/\sqrt{\varepsilon})$ contributions). Also given in Table I are values for an estimate for a_0 (\bar{a}_0). This is generated by assuming that $\kappa_x = \bar{a}_0$ is constant and then considering Eq. (5.10) for $x = 0$:

$$\bar{a}_0 = \frac{4}{3} \sigma_c \gamma \int_\varepsilon^\Lambda \frac{dy}{\sqrt{y} \sqrt{y + \bar{a}_0}} \approx \frac{4}{3} \sigma_c \gamma \ln \left(\frac{4\Lambda}{\bar{a}_0} \right). \quad (5.17)$$

This estimate is useful for understanding the Λ -dependence of the full solution κ_x . \bar{a}_0 scales *almost* logarithmically with Λ , but not quite; the same is true for κ_x . Empirically, we find that

$$\bar{\kappa}(x') = \kappa(x = x' a_0(\Lambda); \Lambda) - a_0(\Lambda) \quad (5.18)$$

is independent of Λ , shown in Fig. 4.

The appearance of the scaled argument $x' = x/a_0(\Lambda)$ in Eq. (5.18) may at first seem somewhat arbitrary. We have seen that the presence of the σ_c/\bar{k}^4 term in the Coulomb kernel leads to the existence of an infrared mass scale a_0

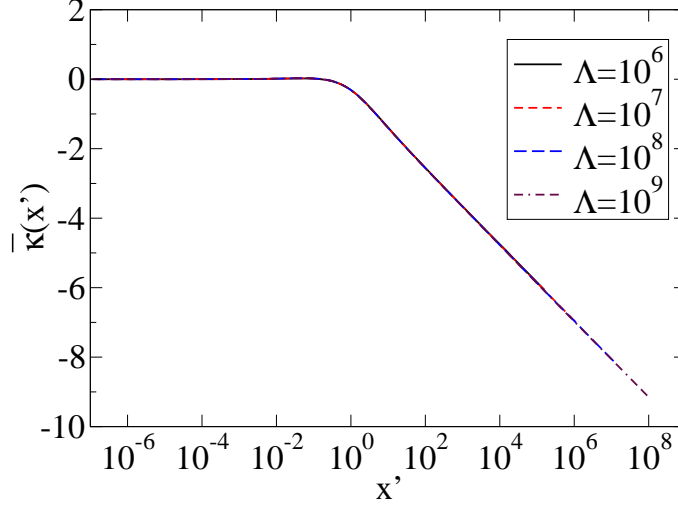


FIG. 4: Plot of $\bar{\kappa}(x')$ for various values of the UV-cutoff, Λ . All dimensionful quantities are in units of σ_c . See text for details.

that is generated by the regularization scale Λ . The process of renormalization is tantamount to choosing a reference scale, relative to which all other quantities are expressed. Importantly, both the function κ_x and the string tension σ_c have dimension $[mass]^2$ and must therefore be measured in the appropriate units. Choosing the (nonperturbatively generated) scale $a_0(\Lambda)$ as our reference scale (thereby implicitly choosing the renormalization subtraction point $\mu = 0$ as will be seen below), we can rewrite the original equation for κ_x , Eq. (5.10), in terms of rescaled quantities. Restoring the putative string tension, σ_c , and denoting all scaled quantities with a prime:

$$x' = \frac{x}{a_0(\Lambda)}, \quad \sigma'_c = \frac{\sigma_c}{a_0(\Lambda)}, \quad \kappa' = \frac{\kappa}{a_0(\Lambda)}, \dots \quad (5.19)$$

(similarly for y , θ , ε and Λ itself), Eq. (5.10) can be rewritten as

$$\kappa'(x'; \sigma'_c, \Lambda') = \sigma'_c \gamma \int_{\varepsilon'}^{\Lambda'} \frac{dy'}{y'} \int_{-1}^1 dz K(x', y'; z) \frac{\theta' - x' + \kappa'(\theta'; \sigma'_c, \Lambda') - \kappa'(x'; \sigma'_c, \Lambda')}{\sqrt{y'} \sqrt{\theta' + \kappa'(\theta'; \sigma'_c, \Lambda')}}. \quad (5.20)$$

Notice that the equation for κ' does not explicitly include reference to $a_0(\Lambda)$: the $a_0(\Lambda)$ -dependence resides in the condition

$$a_0(\Lambda) = \kappa(x=0; \sigma_c, \Lambda) = a_0(\Lambda) \kappa'(x=x' a_0(\Lambda)=0; \sigma_c = \sigma'_c a_0(\Lambda), \Lambda = \Lambda' a_0(\Lambda)) \quad (5.21)$$

(technically, a_0 is also dependent on σ_c , but for notational convenience we shall drop the label) such that one may regard κ' as a function of primed quantities and where $\kappa'(x'=0; \sigma'_c, \Lambda') = 1$. Subtracting at $x' = 0$ and defining

$$\Delta \kappa'(x', 0; \sigma'_c) = \kappa'(x'; \sigma'_c, \Lambda') - \kappa'(0; \sigma'_c, \Lambda') = \kappa'(x'; \sigma'_c, \Lambda') - 1 \quad (5.22)$$

then we arrive at a closed expression for $\Delta \kappa'(x', 0; \sigma'_c)$:

$$\Delta \kappa'(x', 0; \sigma'_c) = \sigma'_c \gamma \int_{\varepsilon'}^{\Lambda'} \frac{dy'}{y'} \left\{ \int_{-1}^1 dz K(x', y'; z) \frac{\theta' - x' + \Delta \kappa'(\theta', 0; \sigma'_c) - \Delta \kappa'(x', 0; \sigma'_c)}{\sqrt{y'} \sqrt{1 + \theta' + \Delta \kappa'(\theta', 0; \sigma'_c)}} - \frac{4}{3} \frac{y' + \Delta \kappa'(y', 0; \sigma'_c)}{\sqrt{y'} \sqrt{1 + y' + \Delta \kappa'(y', 0; \sigma'_c)}} \right\}. \quad (5.23)$$

$\Delta \kappa'(x', 0; \sigma'_c)$ is explicitly independent of Λ' , just as a renormalized quantity should be. It is however dependent on σ'_c , the scaled string tension. We see that, rather than in the unrenormalized case where everything is expressed in units of the string tension, in the renormalized case, everything is expressed in units of an implicit nonperturbatively generated scale.

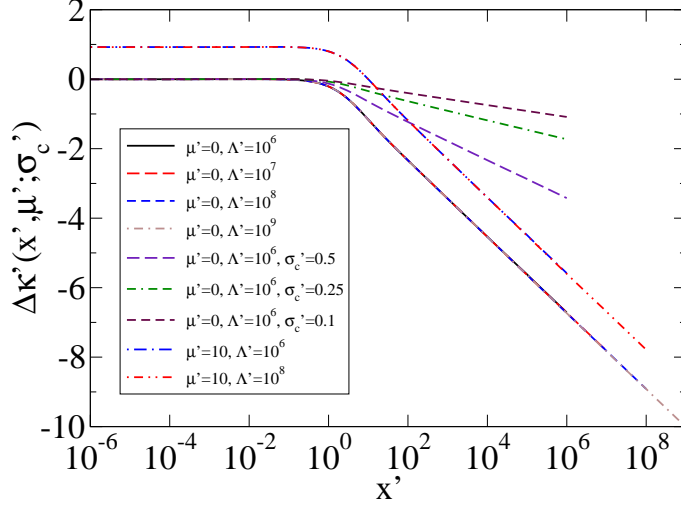


FIG. 5: $\Delta\kappa'(x', \mu'; \sigma'_c)$ for various values of Λ' , σ'_c ($= 1$ unless otherwise stated) and two different μ' . See text for details.

The subtraction at $x = x' = 0$ is not the only possibility. Subtraction at $x' = \mu'$ is also possible and in this case the scale $a(\Lambda) = \kappa(x = \mu' a(\Lambda); \sigma_c, \Lambda)$ is chosen as a reference, such that

$$\Delta\kappa'(x', \mu'; \sigma'_c) = \kappa'(x'; \sigma'_c, \Lambda') - \kappa'(\mu'; \sigma'_c, \Lambda') = \kappa'(x'; \sigma'_c, \Lambda') - 1 \quad (5.24)$$

and which obeys

$$\Delta\kappa'(x', \mu'; \sigma'_c) = \sigma'_c \gamma \int_{\varepsilon'}^{\Lambda'} \frac{dy'}{y'} \left\{ \int_{-1}^1 dz K(x', y'; z) \frac{\theta' - x' + \Delta\kappa'(\theta', \mu'; \sigma'_c) - \Delta\kappa'(x', \mu'; \sigma'_c)}{\sqrt{y'} \sqrt{1 + \theta' + \Delta\kappa'(\theta', \mu'; \sigma'_c)}} - (x' \rightarrow \mu') \right\}. \quad (5.25)$$

The slope of the curves in the UV is proportional to σ'_c and is the same for each value of μ' – the *scaled* string tension σ'_c is independent of the renormalization point, although the scaling factor, $a(\Lambda)$, is dependent on the choice of subtraction point μ' . This is nothing other than the statement that σ'_c is the external input to the renormalized equation. $\Delta\kappa'(x', \mu'; \sigma'_c)$ is plotted in Fig. 5 for various values of Λ' , σ'_c and two different μ' .

We notice that in Fig. 5, the curves for different μ' follow the same pattern as for the unrenormalized case, Fig. 3 with different values of Λ . The following question arises: given $\Delta\kappa'(x', \mu'; \sigma'_c)$, can we derive the renormalized function for a different subtraction point, $\bar{\mu}$, and what are the associated scale factors? To answer the question, let us take a step back to the original unrenormalized function $\kappa(x; \sigma_c, \Lambda)$ and define

$$\begin{aligned} a(\Lambda) &= \kappa(x = \mu' a(\Lambda); \sigma_c = \sigma'_c a(\Lambda), \Lambda = \Lambda' a(\Lambda)), \\ b(\Lambda) &= \kappa(x = \bar{\mu} b(\Lambda); \sigma_c = \bar{\sigma}_c b(\Lambda), \Lambda = \bar{\Lambda} b(\Lambda)). \end{aligned} \quad (5.26)$$

So, knowing the unrenormalized function $\kappa(x; \sigma_c, \Lambda)$, $a(\Lambda)$ and $b(\Lambda)$ can be derived for the chosen μ' and $\bar{\mu}$. Further defining the scaled functions as before:

$$\begin{aligned} \kappa(x; \sigma_c, \Lambda) &= a(\Lambda) \kappa'(x = x' a(\Lambda); \sigma_c = \sigma'_c a(\Lambda), \Lambda = \Lambda' a(\Lambda)), \\ &= b(\Lambda) \bar{\kappa}(x = \bar{x} b(\Lambda); \sigma_c = \bar{\sigma}_c b(\Lambda), \Lambda = \bar{\Lambda} b(\Lambda)), \end{aligned} \quad (5.27)$$

such that when written in terms of the appropriately scaled variables

$$\kappa'(x' = \mu'; \sigma'_c, \Lambda') = \bar{\kappa}(\bar{x} = \bar{\mu}; \bar{\sigma}_c, \bar{\Lambda}) = 1. \quad (5.28)$$

The renormalized (Λ -independent) functions are then

$$\begin{aligned} \Delta\kappa'(x', \mu'; \sigma'_c) &= \kappa'(x = x' a(\Lambda); \sigma_c = \sigma'_c a(\Lambda), \Lambda = \Lambda' a(\Lambda)) - 1, \\ \Delta\bar{\kappa}(\bar{x}, \bar{\mu}; \bar{\sigma}_c) &= \bar{\kappa}(x = \bar{x} b(\Lambda); \sigma_c = \bar{\sigma}_c b(\Lambda), \Lambda = \bar{\Lambda} b(\Lambda)) - 1. \end{aligned} \quad (5.29)$$

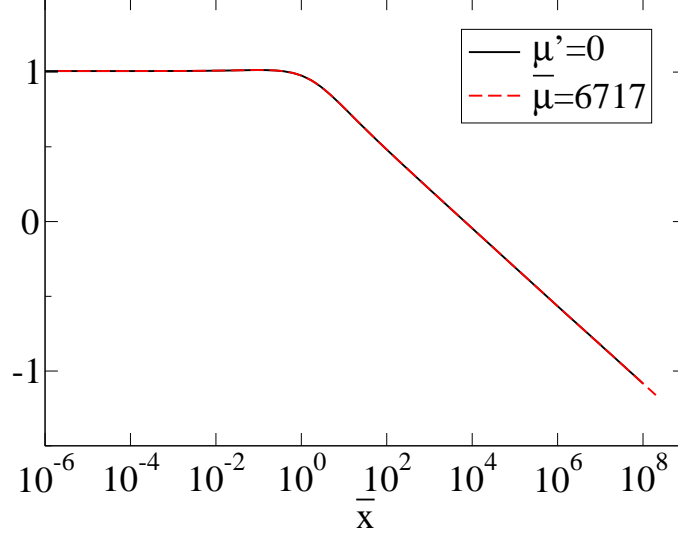


FIG. 6: Renormalized functions $f(\bar{x})$ (labeled as $\mu' = 0$) and $\Delta\bar{\kappa}(\bar{x}, \bar{\mu}; \bar{\sigma}_c)$ (labeled $\bar{\mu} = 6717$) plotted versus \bar{x} . See text for details.

Importantly, both the above functions can be related to the original unrenormalized function κ and the original variables through Eq. (5.27). One thus sees that

$$\Delta\bar{\kappa}(\bar{x}, \bar{\mu}; \bar{\sigma}_c) + 1 = \frac{a(\Lambda)}{b(\Lambda)} \left[\Delta\kappa' \left(x' = \bar{x} \frac{b(\Lambda)}{a(\Lambda)}, \mu'; \sigma'_c = \bar{\sigma}_c \frac{b(\Lambda)}{a(\Lambda)} \right) + 1 \right]. \quad (5.30)$$

So, one can indeed derive the renormalized function for subtraction point $\bar{\mu}$ in terms of that subtracted at μ' and there is a single scale factor given by the ratio

$$Z(\bar{\mu}, \mu'; \sigma_c, \Lambda) = \frac{a(\Lambda)}{b(\Lambda)} = \frac{\kappa(x = \mu' a(\Lambda); \sigma_c, \Lambda)}{\kappa(x = \bar{\mu} b(\Lambda); \sigma_c, \Lambda)}. \quad (5.31)$$

To test this, we take the unrenormalized function with $\sigma_c = 1$, $\Lambda = 10^8$ (plotted in Fig. 3) and consider the case $\mu' = 0$ to give $a(\Lambda) = 8.4679$ and $\sigma'_c = 1/a(\Lambda)$ (implicitly in units of σ_c). Considering $\bar{\mu} = 6.7171 \times 10^3$, the ratio $Z \equiv a(\Lambda)/b(\Lambda) = 2.0067$, with $b(\Lambda) = 4.2198$ and $\bar{\sigma}_c = 1/b(\Lambda)$. The functions

$$f(\bar{x}) \equiv Z [\Delta\kappa'(x' = \bar{x}/Z, \mu' = 0; \sigma'_c = \bar{\sigma}_c/Z) + 1] - 1 \quad (5.32)$$

and $\Delta\bar{\kappa}(\bar{x}, \bar{\mu}; \bar{\sigma}_c)$ are plotted in Fig. 6 and one sees that they are identical (as they should be).

Returning to the dressing function G_x , we see that

$$G_x = G(x; \sigma_c, \Lambda) = \frac{x}{x + \kappa(x; \sigma_c, \Lambda)} = \frac{x'}{x' + 1 + \Delta\kappa'(x', \mu'; \sigma'_c)} = G'(x', \mu'; \sigma'_c). \quad (5.33)$$

When all dimensionful quantities are expressed in terms of the appropriate units (i.e., scaled by the nonperturbatively generated scale defined by the subtraction point μ'), the dressing function G is automatically independent of the UV-cutoff without modification and with a ‘mass function’ $1 + \Delta\kappa'(x', \mu'; \sigma'_c)$ in these units. (The scaling factor $Z(\bar{\mu}, \mu'; \sigma_c, \Lambda)$, defined in terms of the unrenormalized solution $\kappa(x; \sigma_c, \Lambda)$, tells us how the physical scale varies with different renormalization points.) In other words, the gluon dressing function requires no renormalization factor once the physical scale has been set. This has the implication that the nonperturbatively generated gluon mass would be an observable under the present truncation and with the $1/\bar{q}^4$ interaction, despite the naive appearance of a logarithmic UV-divergence.

B. quark gap equation

As in the case for the gluon gap equation, it is convenient to change the momentum routing in the quark gap equation, Eq. (4.23), such that the radial integration momentum goes through the Coulomb kernel. The corresponding equation is then

$$M_k = m + 4\pi\sigma_c \int \frac{d\vec{\omega}}{[\vec{\omega}^2 + \xi]^2 \left[(\vec{k} - \vec{\omega})^2 + M_{k-\omega}^2 \right]^{1/2}} \left[M_{k-\omega} - \frac{\vec{k} \cdot (\vec{k} - \vec{\omega})}{\vec{k}^2} M_k \right] \quad (5.34)$$

where we have inserted the second form for the Coulomb kernel, Eq. (3.19): an infrared regularized form for the interaction with ξ having dimension $[mass]^2$ and playing the role of a fictitious mass scale and for which the limit $\xi \rightarrow 0$ will be studied. (This is the infrared regularization method used, for example, in Ref. [39].) As has been emphasized, one can see the obvious similarities between the gluon and quark gap equations. In fact, there are some subtle differences arising from the specific forms for the integral kernel: in the quark case, the infrared singularities are somewhat more difficult to overcome than in the gluon case; however, the quark equation is explicitly UV-convergent with the above interaction. Notice that we will use the original form for the string tension, σ_c , without mentioning the renormalization and scaling factors arising from the discussion of the gluon. For the quark case, all results may be expressed in units of σ_c directly (as shall be seen) and one may use σ_c or σ'_c interchangeably as input. Using the conventions for the variables as for the gluon equation whereby $\vec{k}^2 = x$, etc., the equation reads

$$M_x = m + \frac{\sigma_c}{2\pi} \int_{\varepsilon}^{\Lambda} \frac{dy \sqrt{y}}{[y + \xi]^2} \int_{-1}^1 \frac{dz}{[\theta + M_{\theta}^2]^{1/2}} \left[M_{\theta} - M_x + \sqrt{\frac{y}{x}} z M_x \right]. \quad (5.35)$$

In the above equation, a second possibility for infrared regularization emerges: one can set $\xi = 0$ and study the infrared cutoff limit $\varepsilon \rightarrow 0$ instead of the infrared mass regularization. It will be seen that both methods give identical results.

The infrared analysis of Eq. (5.35) follows in the same manner as for the gluon. Setting $\xi = 0$ for the moment it follows that for the radial integral to converge as $y \rightarrow 0$, there must be some cancellation within the angular integral and we require that

$$I_z(x, y) = \int_{-1}^1 \frac{dz}{[\theta + M_{\theta}^2]^{1/2}} \left[M_{\theta} - M_x + \sqrt{\frac{y}{x}} z M_x \right] \quad (5.36)$$

vanishes fast enough in this limit, and for all values of x . Using the techniques as before, this is clearly achieved if M_x tends to a constant in the infrared (and as will be seen numerically).

The UV analysis is best performed perturbatively. Consider the following integral (restoring here the original variables, \vec{k} , etc.):

$$I = m + 4\pi\sigma_c M_0 \int \frac{d\vec{\omega}}{[\vec{\omega}^2]^2 \left[(\vec{k} - \vec{\omega})^2 + M_0^2 \right]^{1/2}} \frac{\vec{k} \cdot \vec{\omega}}{\vec{k}^2} \quad (5.37)$$

which corresponds to the case of Eq. (5.34) where $\xi = 0$ and where the function M within the integrand has been replaced by a constant, M_0 (i.e., the above integral represents a first iteration of the full gap equation). The above integral can be performed using dimensional regularization (see, for example, Refs. [18, 20] for a discussion of such integrals) and the result for $\vec{k}^2 \gg M_0^2$ is

$$I \stackrel{\vec{k}^2 \gg M_0^2}{\approx} m + \frac{\sigma_c M_0}{\pi \vec{k}^2} + \mathcal{O}(1/\vec{k}^4). \quad (5.38)$$

Importantly, the integral is explicitly UV-convergent (for all external momenta, \vec{k}^2) and this means that the solution to the quark gap equation requires no renormalization, at least in the absence of the perturbative interaction $\sim 1/\vec{k}^2$. Unlike the gluon, the nonperturbatively generated dynamical scale thus plays no role in setting the physical units. In the full equation, Eq. (5.34), one would expect that the mass function vanishes in the UV like $1/\vec{k}^2$ when the bare quark mass $m \neq 0$, since within the integrand, the mass function is negligible compared to the large momentum. In the chiral case, $m = 0$, one would expect that the mass function vanishes faster than $1/\vec{k}^2$.

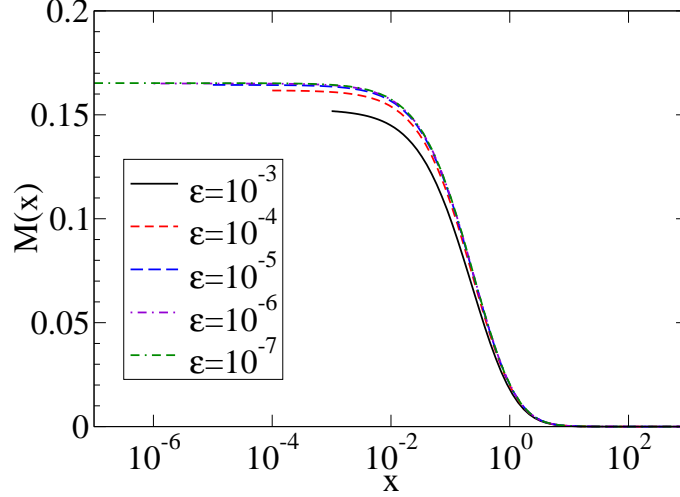


FIG. 7: Chiral quark mass function, M_x , plotted for varying infrared cutoff regulator ε . All dimensionful quantities are in appropriate units of the string tension, σ_c . See text for details.

Having discussed the asymptotic behavior, let us now turn to the numerical solution of Eq. (5.35). In the presence of the infrared singular integrals, it is again necessary to modify the equation for numerical use. To iterate, we use the form

$$M_x = \frac{m + I_1(x; \varepsilon, \xi, \Lambda)}{1 + I_2(x; \varepsilon, \xi, \Lambda)} \quad (5.39)$$

where

$$\begin{aligned} I_1(x; \varepsilon, \xi, \Lambda) &= \frac{\sigma_c}{2\pi} \int_{\varepsilon}^{\Lambda} \frac{dy \sqrt{y}}{[y + \xi]^2} \int_{-1}^1 \frac{dz M_{\theta}}{[\theta + M_{\theta}^2]^{1/2}} \\ I_2(x; \varepsilon, \xi, \Lambda) &= \frac{\sigma_c}{2\pi} \int_{\varepsilon}^{\Lambda} \frac{dy \sqrt{y}}{[y + \xi]^2} \int_{-1}^1 \frac{dz}{[\theta + M_{\theta}^2]^{1/2}} \left[1 - \sqrt{\frac{y}{x}} z \right] \end{aligned} \quad (5.40)$$

and we will consider two cases for the infrared regularization: $\varepsilon \rightarrow 0$ with $\xi = 0$ (infrared cutoff) and $\xi \rightarrow 0$ with $\varepsilon \ll \xi$ (infrared mass). The iteration procedure for Eq. (5.39) is stable over a range of values for ξ and ε , but becomes progressively more difficult as the regulators are made smaller and where the integrals diverge as $1/\sqrt{\varepsilon}$ or $1/\sqrt{\xi}$. The integrals are performed as for the gluon, the only difference being the asymptotic formula in the UV, where a powerlaw form

$$M_x \stackrel{x \rightarrow \Lambda}{\sim} m + cx^{-d} \quad (5.41)$$

is used. Setting $\sigma_c = 1$, all dimensionful quantities are henceforth expressed in units of σ_c (or σ'_c if one uses the renormalized scale defined via the massive gluon propagator). Note that the number of colors, N_c , has already been absorbed into the definition of the Coulomb kernel. Typically, the solutions to Eq. (5.39) are stable for $\Lambda = 10^3$ in the chiral case and $\Lambda = 10^4$ for the massive case (the only exception is the heaviest mass $m = 10$, for which $\Lambda = 10^5$ is necessary, see later for details).

Starting with the chiral quark ($m = 0$) and with infrared cutoff regularization (i.e., studying the limit $\varepsilon \rightarrow 0$ with $\xi = 0$), the quark mass function, M_x , is plotted in Fig. 7 for various values of ε . One sees that as $\varepsilon \rightarrow 0$, the mass function goes to a constant value $M(x=0) = M_0 \approx 0.165$ (in units of $\sqrt{\sigma_c}$) in the IR. The solution thus corresponds to a situation whereby chiral symmetry is dynamically broken. Numerically, the behavior in the UV corresponds to a powerlaw with exponent $d \approx 1.84$ (for the lowest value of ε), which we shall discuss shortly.

Repeating the analysis for the chiral quark, but with an infrared mass regularization (i.e., studying the limit $\xi \rightarrow 0$, with $\varepsilon < 10^{-8} \ll \xi$), the solution is plotted in Fig. 8 for various values of ξ . It is seen that as the regularization is removed, the mass function becomes identical to that using the infrared cutoff method, showing that the two methods

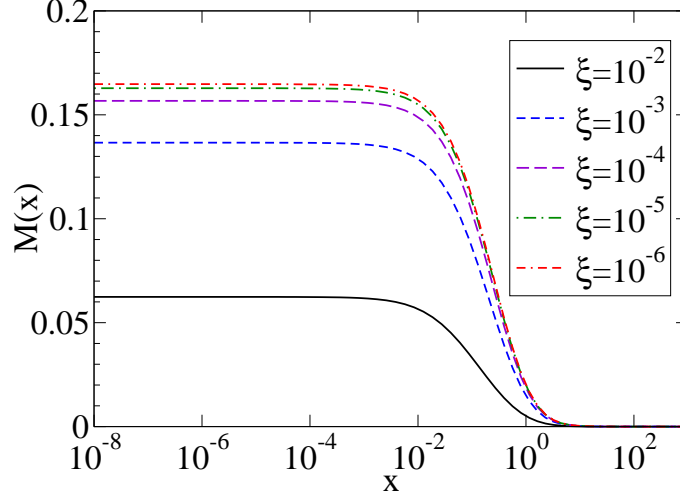


FIG. 8: Chiral quark mass function, M_x , plotted for varying infrared mass regulator ξ . All dimensionful quantities are in appropriate units of the string tension, σ_c . See text for details.

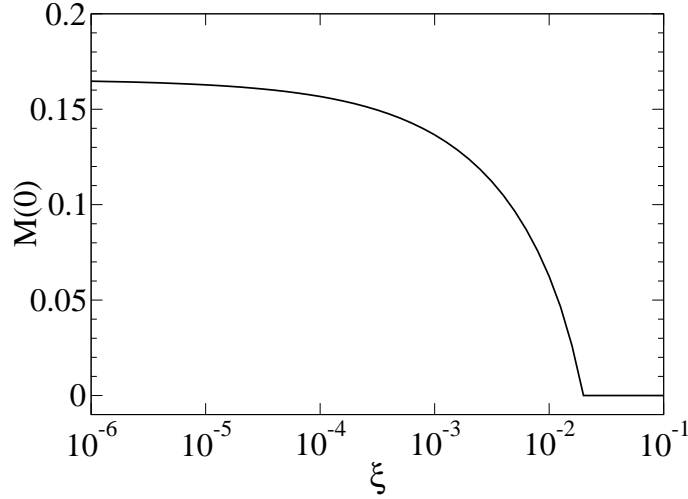


FIG. 9: Chiral quark mass function at zero momentum, $M(x=0)$, plotted as a function of the infrared mass regulator ξ . All dimensionful quantities are in appropriate units of the string tension, σ_c . See text for details.

agree. The infrared constant value is the same as before $M_0 \approx 0.165$, although the UV exponent is a little larger: $d \approx 1.90$. Both sets of results for the chiral quark may be directly compared to those of Ref. [39] or, allowing for a factor $C_F = 4/3$ in the definition of σ_c , to the results of Refs. [11, 12]. Turning to the UV exponent, Ref. [12] showed that one should expect $d = 2$ (in other words $M \sim 1/\vec{k}^4$ in the UV). The numerical results here are somewhat lower (although within a reasonable numerical precision); however, given that the function is vanishing so rapidly, the effect of the UV tail is negligible.

The behavior of the mass function for varying infrared mass regulator is rather interesting. In Fig. 9, the infrared constant mass, M_0 , is plotted as a function of ξ . It is seen that as $\xi \rightarrow 0$, M_0 tends to its constant, nonzero value and indicating that chiral symmetry is dynamically broken in the presence of the strongly infrared enhanced Coulomb kernel interaction (and which one would naively expect). However, what is also seen is that for large ξ , M_0 rapidly decreases and vanishes altogether for $\xi > 0.02$. As is well known, the interaction $F \sim \sigma_c/\vec{k}^4$ corresponds to a linearly

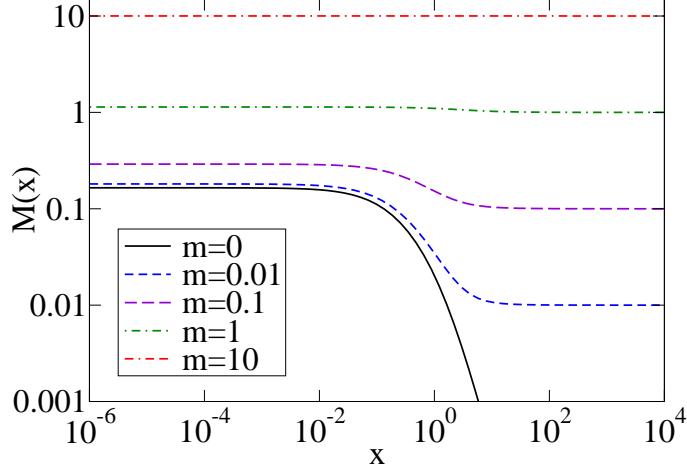


FIG. 10: Quark mass function, M_x , plotted for various bare quark masses. All dimensionful quantities are in appropriate units of the string tension, σ_c . See text for details.

rising potential with a coefficient given by σ_c . The explicit expression, appropriate to Coulomb gauge in the heavy quark limit and under the truncation to neglect pure Yang-Mills vertices reads [23] (temporarily reinstating the string tension σ_c and all other constants):

$$V(r) = g^2 C_F \int d\vec{\omega} \tilde{F}_\omega (1 - e^{i\vec{\omega} \cdot \vec{r}}) = \int d\vec{\omega} \left\{ \mathcal{C} (2\pi)^3 \delta(\vec{\omega}) + \frac{8\pi\sigma_c}{[\vec{\omega}^2 + \xi]^2} \right\} (1 - e^{i\vec{\omega} \cdot \vec{r}}) \quad (5.42)$$

where r is a length scale. We shall shortly show that this form is indeed the correct expression for the truncation scheme considered here. The δ -function term proportional to \mathcal{C} arises from the charge conservation term originating in resolving the temporal zero modes inherent to Coulomb gauge. This term does not contribute to the potential: such a term was in fact considered in Ref. [12], to the same effect. With the infrared mass regularization, the integral is

$$V(r) = \frac{\sigma_c}{\sqrt{\xi}} \left[1 - e^{-r\sqrt{\xi}} \right] = \begin{cases} \sigma_c r, & r\sqrt{\xi} \rightarrow 0 \\ \sigma_c / \sqrt{\xi}, & r\sqrt{\xi} \rightarrow \infty. \end{cases} \quad (5.43)$$

In the limit $\xi \rightarrow 0$ and for finite length scale r , $V(r)$, is a good approximation to the linearly rising potential, which gets better as ξ decreases. However, as ξ increases (whilst keeping r fixed), $V(r)$ flattens to a constant and this constant decreases as ξ increases. The restoration of chiral symmetry for large ξ is now rather obvious – for large ξ , the long-range part of the potential is no longer linearly-rising, but is constant. Thus, within the truncation scheme here, chiral symmetry is always broken by the existence of a pure linearly rising potential, the dynamically generated quark mass being measured in units of $\sqrt{\sigma_c}$. One cannot speak of a critical string tension in this respect (as compared to the concept of a critical coupling). However, the dynamical breaking of chiral symmetry is sensitive to the details of the potential when there is a flattening at large range, caused in this case by the large value of the infrared mass regulator.

Let us finally discuss the case when the quarks have a nonzero bare mass. In the absence of UV-divergences, the bare mass requires no corrections due to renormalization. We again set $\sigma_c = 1$ such that all dimensionful quantities are measured in the appropriate unit of the string tension. Using the infrared cutoff method, with $\varepsilon = 10^{-6}$ and $\Lambda = 10^4$ (except for the case $m = 10$, where $\Lambda = 10^5$ is used), the solution to the gap equation for various quark masses is shown in Fig. 10 (the chiral quark is shown for comparison). One sees that in all cases, the quark mass function is constant in the infrared. In the UV, the exponent of the powerlaw lies in the range $d = 1.02 - 1.07$. This is comparable to the expected value $d = 1$ obtained earlier from the perturbative analysis, though as for the chiral quarks, the UV tail is not particularly important. In Fig. 11, we plot the deviation of the mass function from the bare quark mass: $M_x - m$. Two features emerge from this plot. The first is that as m increases, the infrared constant value $M_0 - m$ extends further into the UV region (this is why Λ must be increased for the largest value of m , such that the solution converges properly). The second feature is that for increasing bare mass, m , the difference of the

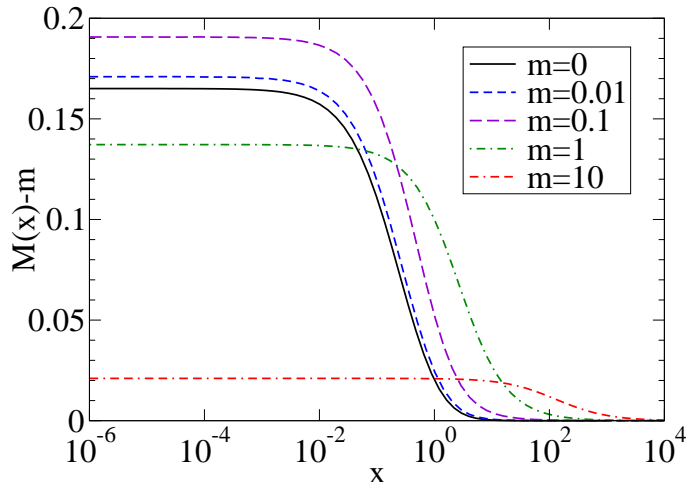


FIG. 11: Difference of the quark mass function and the bare quark mass, $M_x - m$, plotted for various bare quark masses. All dimensionful quantities are in appropriate units of the string tension, σ_c . See text for details.

infrared value $M_0 - m$ initially increases, but then turns over such that for heavy quarks, this difference becomes significantly smaller. In the heavy quark limit, one thus sees that $M_x - m$ is suppressed, at least in this truncation. Moreover, as the difference $M_x - m$ vanishes when $m \rightarrow \infty$, then the question of the ordering of the limits $m \rightarrow \infty$ and $\Lambda \rightarrow \infty$ becomes irrelevant. One can thus see that the relation Eq. (4.27) is valid such that the connection between the truncated quark gap equation studied in this work and the heavy quark limit studied analytically in Refs. [23–25] (where contributions from pure Yang-Mills vertices were neglected) is established. This justifies the earlier use of Eq. (5.42).

VI. SUMMARY, DISCUSSION AND CONCLUSIONS

In this study, we have considered Coulomb gauge quantum chromodynamics within the first order formalism, under a leading order truncation and concentrating on the infrared behavior. In fixing to Coulomb gauge, particular attention must be paid to the temporal zero modes of the Faddeev-Popov operator. Within the first order formalism in Coulomb gauge, the temporal component of the gauge field can be exactly integrated out, leading to the cancellation of the Faddeev-Popov determinant; what remains of the gluon sector concerns two transverse field degrees of freedom \vec{A} and $\vec{\pi}$. The resolution of the temporal zero modes further leads to the constraint that the total color charge be conserved and vanishing. This constraint was written in Gaussian form, resulting in a constant shift in the Coulomb kernel, proportional to $\mathcal{C} \rightarrow \infty$.

Having integrated out the temporal component of the gluon field, the action is nonlocal due to the presence of the inverse Faddeev-Popov operator occurring in the Coulomb kernel. In order to derive the Dyson-Schwinger equations, a leading order truncation was introduced whereby the nonlocal Coulomb kernel was replaced by its expectation value in the form of an input Ansatz. This truncation led to the appearance of a set of new (momentum dependent) four-point interaction vertices. These vertices effectively replace the dynamical content of the tower of Dyson-Schwinger equations and Slavnov-Taylor identities involving the temporal, longitudinal and ghost degrees of freedom in the local formalism. The resulting Dyson-Schwinger equations were further truncated to include (and subsequently study) only those one-loop tadpole terms involving the nonperturbative part of the input Ansatz for the Coulomb kernel, which was taken to be strongly infrared enhanced ($\sim 1/\vec{k}^4$).

It was found that the truncated equation for the mixed gluonic proper two-point function, $\Gamma_{\pi A}$, leads immediately to the result that this component is trivial. This in turn meant that in the subsequent gluonic Dyson-Schwinger equations for $\Gamma_{\pi\pi}$ and Γ_{AA} , the energy dependence could be resolved. Moreover, the static gluon propagators could be easily identified in terms of a single dressing function, G . The proper two-point dressing functions were dependent on the constant \mathcal{C} (arising from the charge constraint) and included potentially infrared divergent integral contributions (see below for a discussion). However, combining the two Dyson-Schwinger equations led to an equation for G alone: Eq. (4.12). This “gluon gap equation” for the static dressing function G was independent of \mathcal{C} and (as was numerically

verified) had a finite solution, despite the strongly infrared singular interaction. An almost identical situation was seen for the quark sector: the static propagator was given in terms of a single dressing function, M , and a gap equation arose, Eq. (4.23), which was independent of \mathcal{C} and whose solution was finite, despite the fact that the Dyson-Schwinger equations for the proper dressing functions were explicitly dependent on \mathcal{C} and involved infrared divergent integrals. Importantly, the static gluon and quark gap equations were identical in form to their counterparts derived in the canonical Hamiltonian approach [6, 12]. This allows for an equivalence to be established between the respective truncation schemes and approximations employed within the two approaches.

Using spin projectors, it was possible to consider the heavy quark limit and it was seen that the (full, not static) quark propagator reduces to the known result [23] within this truncation. This is important because in the heavy quark limit, the role of the infrared divergent integrals is understood: when studying physical, color singlet quantities, such infrared divergences cancel whereas for propagators, the pole position is shifted to infinity and reflecting the fact that infinite energy is required for an unphysical colored object to exist in isolation. This in turn explains the constant, \mathcal{C} , stemming from the charge constraint: it is merely an additional, fully nonperturbative and constant contribution to be added to the infrared divergence. Given that the input Ansatz for the Coulomb kernel was shown to be directly related to the instantaneous part of the temporal gluon propagator, which in Ref. [23] was shown to be related to the quark-antiquark potential, \mathcal{C} is simply a constant shift of this potential. In Ref. [12], it was demonstrated that an arbitrary, constant shift in the potential has no observable consequence (at least as far as the chiral quarks studied therein were concerned). Here, the charge constraint arising from the incompleteness of the gauge fixing (the temporal zero modes) results in exactly such an unobservable, constant shift (considering the limit $\mathcal{C} \rightarrow \infty$) in the potential, leaving physical quantities untouched and naively prohibiting unphysical, color charged quantities from existing in isolation (in the sense that infinite energy is required to create such an object).

For both the gluonic and quark sectors, it was numerically found that given the infrared enhanced input Ansatz, the static propagator dressing functions exhibited the presence of a nonperturbatively generated dynamical mass scale. Both functions were nontrivially finite and constant in the infrared. In the case of the gluon, despite the absence of the perturbative components, a logarithmic ultraviolet divergence emerged. However, expressing the gluon gap equation in terms of the nonperturbatively generated dynamical scale, the dressing function was seen to require no renormalization. This would suggest that the dynamical gluon mass would be observable within this leading order truncation insofar as the renormalization is concerned (i.e., if one were to ignore the previous discussion about the charge constraint and infrared divergences connected to the full propagator). The result is in disagreement with the Gribov-Zwanziger confinement scenario [1–3] and the results of Ref. [36]. This is presumably a shortcoming of the leading order truncation scheme utilized in this study.

In the case of the static quark propagator in the chiral limit, the gap equation was solved using two infrared regularization procedures and their equivalence was numerically demonstrated. The results are identical to previous studies [11, 12, 39]. The nonperturbatively generated mass scale corresponds to dynamical chiral symmetry breaking, although one should point out that it is long known that quantitatively the resulting chiral condensate is too small [12] (this subject was tackled in Ref. [11]). Of interest however for the chiral quarks, was the infrared mass regularization, where the regularization parameter, ξ , was large: in this case, the nonperturbatively generated scale decreased as ξ increased and eventually disappeared. Utilizing the connection between the input Ansatz for the interaction and the quark-antiquark potential, the observed restoration of chiral symmetry could be intuitively explained as a flattening of the long-range part of the potential when the interaction is regularized. With heavy quarks, it was explicitly verified numerically that in this truncation, the heavy quark limit emerges naturally.

Clearly, despite the fact that we retain only the leading order contributions and that the input Ansatz for the Coulomb kernel excludes the perturbative content of the theory, the Dyson-Schwinger equations of Coulomb gauge in the first order formalism represent a powerful tool to study nonperturbative quantum chromodynamics. Equally clearly, one can see that much is missing. For example, it is known from the canonical Hamilton approach that: the inclusion of the ghost loop (‘curvature’) in the deep infrared region [8, 9] and the triple-gluon vertex in the mid-momentum region [10] of the static gluon propagator have important roles; also that the spatial quark-gluon vertex is necessary to obtain a reasonable estimate for the chiral quark condensate [11]. Now, in the canonical Hamiltonian approach, the truncation scheme is defined by an initial Ansatz for the vacuum wavefunctional, thereafter it is a matter of computational effort to obtain results. In comparison, the Dyson-Schwinger equations can be derived completely (in the sense that, in principle, all loop terms can be written down) but must subsequently be truncated in order to furnish useful equations. Having made the connection between the two approaches at leading order here, it seems promising that beyond leading order such comparison may provide useful insights into both approaches.

The heavy quark limit of the Dyson-Schwinger equations in Coulomb gauge also seems a very promising avenue for further study. From the lattice, it is known that the physical, Wilson string tension is not simply the coefficient of the infrared singularity in the instantaneous temporal gluon propagator (see, for example, Ref. [33]). The Coulomb string tension is analytically known to be larger than the Wilson string tension, encapsulated in the statement: “No confinement without Coulomb confinement.” [34]. Combining the heavy quark limit of the Dyson-Schwinger equations

beyond the leading order truncation presented here with the Bethe-Salpeter equation, one may hope to study the quark-antiquark potential quantitatively. Thereafter, phenomenological application to the hadron spectrum would be a realistic proposition.

Acknowledgments

The authors gratefully acknowledge useful discussions with G. Burgio and M. Pak. This work has been supported by the Deutsche Forschungsgemeinschaft (DFG) under contracts no. DFG-Re856/6-2,3.

-
- [1] V. N. Gribov, Nucl. Phys. **B139** (1978) 1.
 - [2] D. Zwanziger, Nucl. Phys. **B485**, 185-240 (1997). [hep-th/9603203].
 - [3] D. Zwanziger, Nucl. Phys. **B518** (1998) 237-272.
 - [4] A. Szczepaniak, E. S. Swanson, C. -R. Ji, S. R. Cotanch, Phys. Rev. Lett. **76**, 2011-2014 (1996). [hep-ph/9511422].
 - [5] F. J. Llanes-Estrada, S. R. Cotanch, P. J. de A. Bicudo, J. E. F. T. Ribeiro, A. P. Szczepaniak, Nucl. Phys. **A710**, 45-54 (2002). [hep-ph/0008212].
 - [6] A. P. Szczepaniak, E. S. Swanson, Phys. Rev. **D65** (2002) 025012. [hep-ph/0107078].
 - [7] A. P. Szczepaniak, Phys. Rev. **D69** (2004) 074031. [hep-ph/0306030].
 - [8] C. Feuchter, H. Reinhardt, Phys. Rev. **D70** (2004) 105021. [hep-th/0408236].
 - [9] H. Reinhardt, C. Feuchter, Phys. Rev. **D71** (2005) 105002. [hep-th/0408237].
 - [10] D. R. Campagnari, H. Reinhardt, Phys. Rev. **D82** (2010) 105021. [arXiv:1009.4599 [hep-th]].
 - [11] M. Pak, H. Reinhardt, [arXiv:1107.5263 [hep-ph]].
 - [12] S. L. Adler, A. C. Davis, Nucl. Phys. **B244** (1984) 469.
 - [13] D. Schutte, Phys. Rev. **D31** (1985) 810-821.
 - [14] N. H. Christ and T. D. Lee, Phys. Rev. D **22**, 939 (1980) [Phys. Scripta **23**, 970 (1981)].
 - [15] P. Watson, H. Reinhardt, Phys. Rev. **D75** (2007) 045021. [hep-th/0612114].
 - [16] K. Lichtenegger, D. Zwanziger, [arXiv:0911.5435 [hep-ph]].
 - [17] R. Alkofer, A. Maas, D. Zwanziger, Few Body Syst. **47**, 73-90 (2010). [arXiv:0905.4594 [hep-ph]].
 - [18] P. Watson, H. Reinhardt, Phys. Rev. **D76** (2007) 125016. [arXiv:0709.0140 [hep-th]].
 - [19] P. Watson, H. Reinhardt, Phys. Rev. **D77** (2008) 025030. [arXiv:0709.3963 [hep-th]].
 - [20] C. Popovici, P. Watson, H. Reinhardt, Phys. Rev. **D79** (2009) 045006. [arXiv:0810.4887 [hep-th]].
 - [21] P. Watson, H. Reinhardt, Eur. Phys. J. **C65** (2010) 567-585. [arXiv:0812.1989 [hep-th]].
 - [22] H. Reinhardt and P. Watson, Phys. Rev. D **79**, 045013 (2009) [arXiv:0808.2436 [hep-th]].
 - [23] C. Popovici, P. Watson, H. Reinhardt, Phys. Rev. **D81** (2010) 105011. [arXiv:1003.3863 [hep-th]].
 - [24] C. Popovici, P. Watson, H. Reinhardt, Phys. Rev. **D83** (2011) 025013. [arXiv:1010.4254 [hep-ph]].
 - [25] C. Popovici, P. Watson, H. Reinhardt, Phys. Rev. **D83** (2011) 125018. [arXiv:1103.4786 [hep-ph]].
 - [26] A. Cucchieri, D. Zwanziger, Phys. Rev. **D65** (2001) 014002. [hep-th/0008248].
 - [27] A. Cucchieri, D. Zwanziger, Phys. Rev. **D65** (2001) 014001. [hep-lat/0008026].
 - [28] K. Langfeld, L. Moyaerts, Phys. Rev. **D70** (2004) 074507. [hep-lat/0406024].
 - [29] A. Cucchieri, A. Maas, T. Mendes, Mod. Phys. Lett. **A22** (2007) 2429-2438. [hep-lat/0701011].
 - [30] M. Quandt, G. Burgio, S. Chimchinda, H. Reinhardt, PoS **CONFINEMENT8** (2008) 066. [arXiv:0812.3842 [hep-th]].
 - [31] Y. Nakagawa, A. Nakamura, T. Saito, H. Toki, PoS **LAT2009** (2009) 230. [arXiv:0911.2550 [hep-lat]].
 - [32] Y. Nakagawa, A. Nakamura, T. Saito, H. Toki, Phys. Rev. **D83** (2011) 114503. [arXiv:1105.6185 [hep-lat]].
 - [33] T. Iritani, H. Suganuma, Phys. Rev. **D83** (2011) 054502. [arXiv:1102.0920 [hep-lat]].
 - [34] D. Zwanziger, Phys. Rev. Lett. **90**, 102001 (2003). [hep-lat/0209105].
 - [35] E. Eichten, F. Feinberg, Phys. Rev. **D23** (1981) 2724.
 - [36] D. Zwanziger, Nucl. Phys. **B364** (1991) 127-161.
 - [37] W. Schleifenbaum, M. Leder and H. Reinhardt, Phys. Rev. D **73**, 125019 (2006) [hep-th/0605115].
 - [38] P. Watson, H. Reinhardt, Phys. Rev. **D82** (2010) 125010. [arXiv:1007.2583 [hep-th]].
 - [39] R. Alkofer, M. Klok, A. Krassnigg, R. F. Wagenbrunn, Phys. Rev. Lett. **96** (2006) 022001. [hep-ph/0510028].